UC Irvine
UC Irvine Previously Published Works

Title
Shorter Is Better: The α-(l)-Threofuranosyl Nucleic Acid Modification Improves Stability, Potency, Safety, and Ago2 Binding and Mitigates Off-Target Effects of Small Interfering RNAs.

Permalink
https://escholarship.org/uc/item/4kh3t8d3

Authors
Matsuda, Shigeo
Bala, Saikat
Liao, Jen-Yu
et al.

Publication Date
2023-08-28

DOI
10.1021/jacs.3c04744

Copyright Information
This work is made available under the terms of a Creative Commons Attribution-NonCommercial License, availalbe at https://creativecommons.org/licenses/by-nc/4.0/

Peer reviewed

eScholarship.org Powered by the California Digital Library
University of California

JACS
JOURNAL OF THE AMERICAN CHEMICAL SOCIETY
pubs.acs.org/JACS
Article

Shorter Is Better: The α-(L)-Threofuranosyl Nucleic Acid Modification Improves Stability, Potency, Safety, and Ago2 Binding and Mitigates Off-Target Effects of Small Interfering RNAs

Shigeo Matsuda, Saikat Bala, Jen-Yu Liao, Dhrubajyoti Datta, Atsushi Mikami, Lauren Woods, Joel M. Harp, Jason A. Gilbert, Anna Bisbe, Rajar M. Manoharan, MaryBeth Kim, Christopher S. Theile, Dale C. Guenther, Yongfeng Jiang, Saket Agarwal, Rajanikanth Maganti, Mark K. Schlegel, Ivan Zlatev, Klaus Charisse, Kallanthottathil G. Rajeev, Adam Castoreno, Martin Maier, Maja M. Janas, Martin Egli, John C. Chaput, and Muthiah Manoharan*

Cite This: https://doi.org/10.1021/jacs.3c04744

Read Online

ACCESS | Metrics & More | Article Recommendations | Supporting Information

ABSTRACT: Chemical modifications are necessary to ensure the metabolic stability and efficacy of oligonucleotide-based therapeutics. Here, we describe analyses of the α-(L)-threofuranosyl nucleic acid (TNA) modification, which has a shorter 3′−2′ internucleotide linkage than the natural DNA and RNA, in the context of small interfering RNAs (siRNAs). The TNA modification enhanced nuclease resistance more than 2′-*O*-methyl or 2′-fluoro ribose modifications. TNA-containing siRNAs were prepared as triantennary *N*-acetylgalactosamine conjugates and were tested in cultured cells and mice. With the exceptions of position 2 of the antisense strand and position 11 of the sense strand, the TNA modification did not inhibit the activity of the RNA interference machinery. In a rat toxicology study, TNA placed at position 7 of the antisense strand of the siRNA mitigated off-target effects, likely due to the decrease in the thermodynamic binding affinity relative to the 2′-*O*-methyl residue. Analysis of the crystal structure of an RNA octamer with a single TNA on each strand showed that the tetrose sugar adopts a C4′-*exo* pucker. Computational models of siRNA antisense strands containing TNA bound to Argonaute 2 suggest that TNA is well accommodated in the region kinked by the enzyme. The combined data indicate that the TNA nucleotides are promising modifications expected to increase the potency, duration of action, and safety of siRNAs.

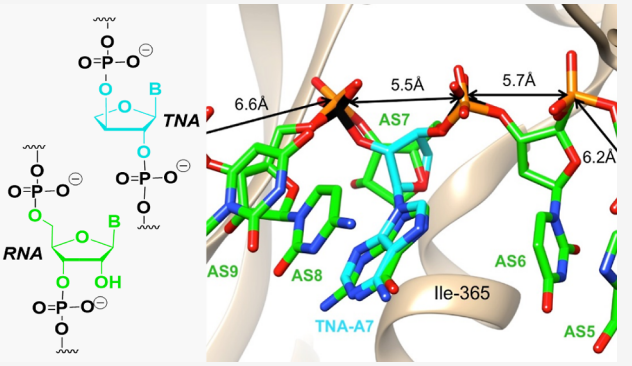

Downloaded via UNIV OF CALIFORNIA IRVINE on August 28, 2023 at 18:33:32 (UTC).
See https://pubs.acs.org/sharingguidelines for options on how to legitimately share published articles.

INTRODUCTION

Oligonucleotide therapeutics such as those based on the RNA interference (RNAi) platform have significant potential to address unmet medical needs. Several RNAi-based therapeutics have been approved for clinical use including patisiran (ONPATTRO), givosiran (GIVLAARI), lumasiran (OXLUMO), inclisiran (LEQVIO), and vutrisiran (AMVUTTRA).[1−7] In each case, appropriate chemical modification and efficient delivery were key to the successful approval.[8−10] Natural RNA duplexes are metabolically unstable, and thus, for use as a therapeutic, the synthetic small interfering RNA (siRNA) must include chemically modified nucleotide-building blocks to prevent enzymatic degradation, to enhance lipophilicity, to improve cell-membrane permeability, and to mitigate immune responses and off-target effects.[11] For example, patisiran contains 2′-*O*-methyl (2′-*O*Me) ribonucleotides and is formulated in lipid nanoparticles,[1] and givosiran, lumasiran, inclisiran, and vutrisiran are chemically modified with 2′-*O*Me and 2′-deoxy-2′-fluoro (2′-F) ribonucleotides and conjugated to a trivalent *N*-acetylgalactosamine (GalNAc, Figure 1A,C,D).[12−14] GalNAc is the ligand for the hepatic asialoglycoprotein receptor. This receptor mediates liver cell-specific uptake of the siRNAs. At most positions in the sense and antisense strands of the siRNA, the 2′-F and 2′-*O*Me modifications are tolerated by Argonaute 2 (Ago2), the catalytic endonuclease component of the RNA-induced silencing complex (RISC).[8,15−18]

Our laboratory has systematically evaluated the role of chemical modifications in siRNA activity with the goals of improving potency, specificity, and safety.[8] The nucleotide at

Received: May 8, 2023

© XXXX American Chemical Society

https://doi.org/10.1021/jacs.3c04744
J. Am. Chem. Soc. XXXX, XXX, XXX−XXX

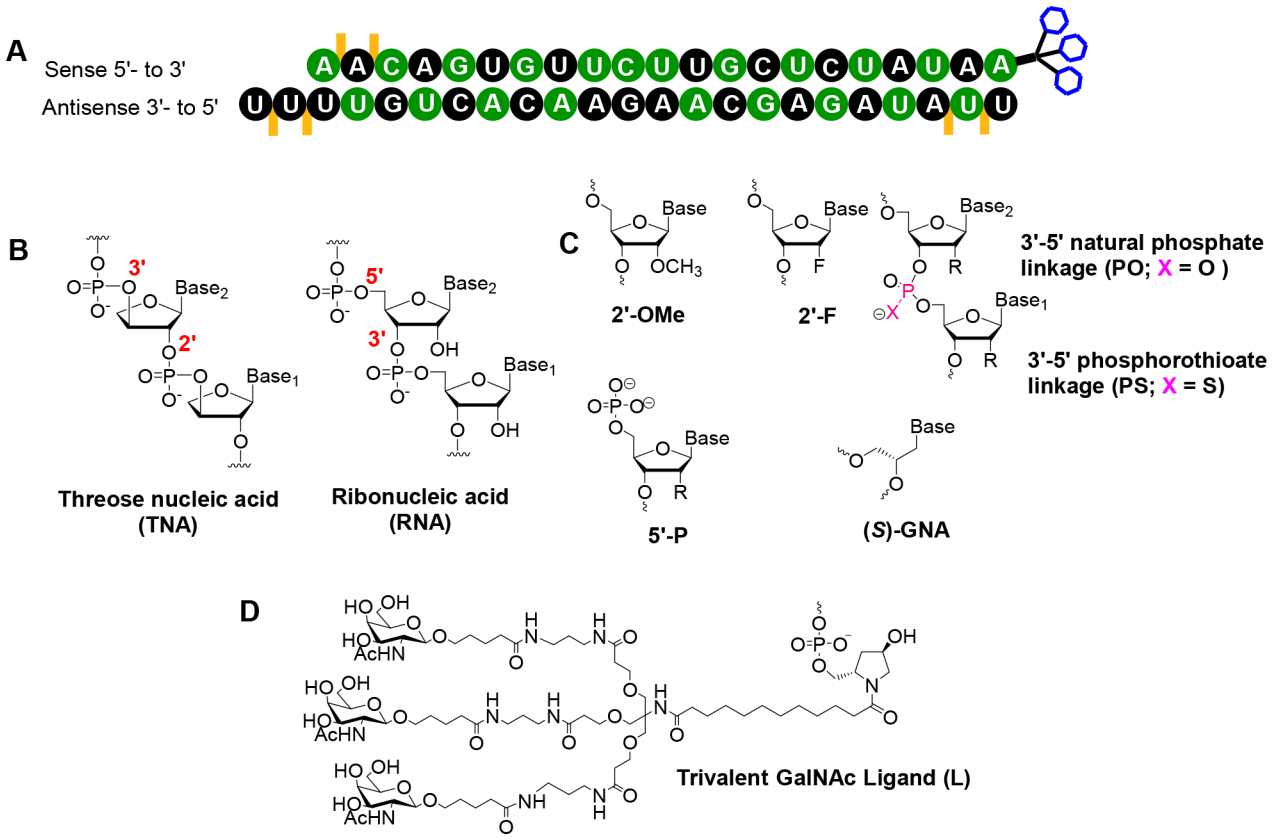

Figure 1. (A) Schematic of the parent siRNA-GalNAc conjugate duplex targeting mouse *Ttr*. This siRNA was previously characterized.[12−14] Black: 2′-*O*Me; green: 2′-F; and orange lines: phosphorothioate linkage. (B) Structures of sugar−phosphate backbones of TNA and RNA. (C) Structures of 2′-*O*Me, 2′-F, natural phosphate and phosphorothioate linkages, 5′-monophosphate, and (*S*)-GNA. (D) Structure of the triantennary GalNAc ligand.

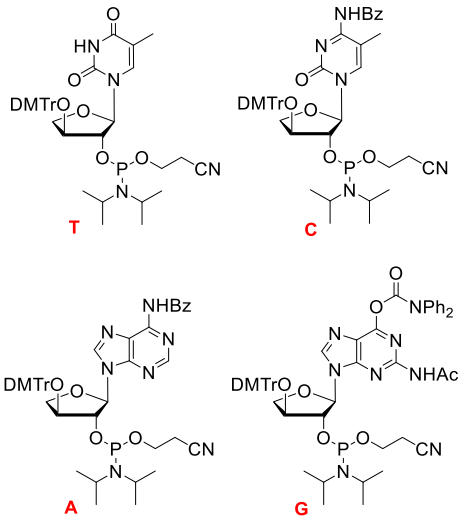

Figure 2. TNA phosphoramidites used in this study.

position 1 of the antisense strand bound to the MID domain of the slicer endonuclease Ago2 adopts a C2′-*endo* or C1′-*exo* (south) conformation, and, thus, the first residue of the siRNA antisense strand can be replaced by 2′-deoxy or 2′-arabino nucleotides.[8] The only nucleotides known to be tolerated at position 2 of the antisense strand are natural nucleotides or 2′-F due to a spatial constraint imposed by Ago2.[8] In the seed region of the antisense strand (positions 2−8), thermodynamically destabilizing modifications, such as unlocked nucleic acid or (*S*)-glycol nucleic acid (GNA, Figure 1C), mitigate off-target effects without reducing gene silencing activity.[13,19−22] The 2′-F modification is well accepted by the RISC, but the nuclease stability provided by this modification is poor.[16] Therefore, we continue to search for modified nucleotides that will enhance the efficacy of therapeutic siRNAs.

Here, we describe the evaluation of siRNAs modified with Professor Albert Eschenmoser's α-(L)-threofuranosyl nucleic acid (TNA, Figure 1B).[23] TNA oligomers are composed of repeating α-L-threofuranosyl nucleotides that are connected by 3′,2′-phosphodiester linkages.[23] TNA is capable of self-pairing and, despite a backbone repeat unit that is one atom shorter than that of DNA and RNA, of cross-pairing with complementary strands of DNA and RNA.[23] The ability to exchange genetic information with RNA, coupled with the chemical simplicity of threose relative to ribose, has led to interest in TNA as a possible RNA progenitor during evolution of life.[23−25] It was the unusual backbone structure, which is recalcitrant to biological nucleases,[26] that motivated researchers to pursue TNA as a synthetic genetic polymer for applications in synthetic biology and biomedicine.[27] With the advent of engineered polymerases,[28] TNA libraries have been queried by in vitro selection for sequences that bind to ligands or that have catalytic activity.[29−33] In the area of synthetic biology, TNA has been used as a biologically secure soft material for low-energy, high-density information storage and data archiving.[34] TNA loops have been used to enhance the delivery and expression of linear DNA genes in eukaryotic cells, which is of relevance to gene therapy.[35] TNA has also been explored as a chemical modality for antisense oligonucleotide therapeutics.[36−39] Preclinical studies indicate that antisense oligonucleotides modified with

https://doi.org/10.1021/jacs.3c04744
J. Am. Chem. Soc. XXXX, XXX, XXX−XXX

Scheme 1. Synthesis of 5-Methyl-C-TNA Phosphoramidite

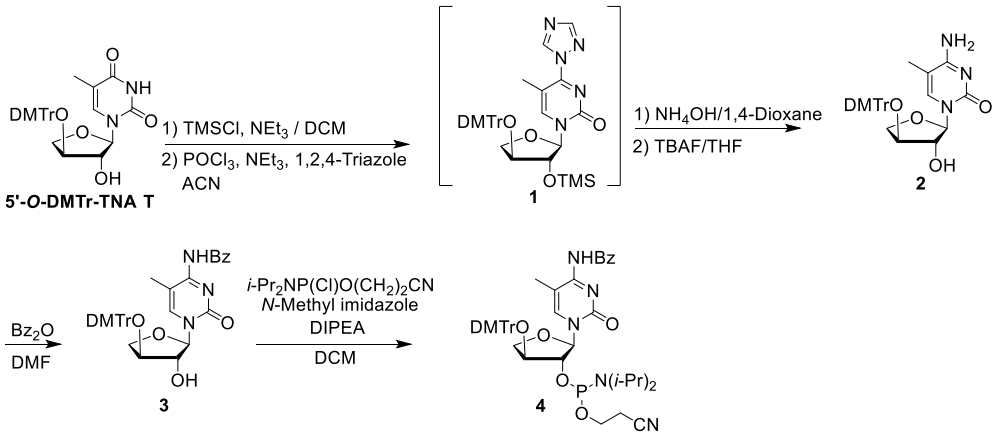

Table 1. Melting Temperatures of RNA Duplexes Modified with TNA or 2′-F[a]

entry	Oligo ID	Sequence[a]	T_m[b] (°C)	ΔT_m[c] (°C)
1	ON1 ON2	5′-r(UACAGUCUAUGU)-3′ 3′-r(AUGUCAGAUACA)-5′	52.6	-
2	ON3 ON2	5′-r(UACAG**T**CUAUGU)-3′ 3′-r(AUGUCAGAUACA)-5′	47.8	-4.8
3	ON4 ON2	5′-r(UACAGU**C**UAUGU)-3′ 3′-r(AUGUCAGAUACA)-5′	47.1	-5.5
4	ON1 ON5	5′-r(UACAGUCUAUGU)-3′ 3′-r(AUGUC**A**GAUACA)-5′	48.1	-4.5
5	ON1 ON6	5′-r(UACAGUCUAUGU)-3′ 3′-r(AUGUCA**G**AUACA)-5′	47.7	-4.9
6	ON3 ON5	5′-r(UACAG**T**CUAUGU)-3′ 3′-r(AUGUC**A**GAUACA)-5′	43.1	-9.5
7	ON4 ON6	5′-r(UACAGU**C**UAUGU)-3′ 3′-r(AUGUCA**G**AUACA)-5′	41.6	-11.0
8	ON7 ON2	5′-r(UACAG***U***CUAUGU)-3′ 3′-r(AUGUCAGAUACA)-5′	53.1	+0.5
9	ON8 ON2	5′-r(UACAGU***C***UAUGU)-3′ 3′-r(AUGUCAGAUACA)-5′	54.3	+1.7
10	ON1 ON9	5′-r(UACAGUCUAUGU)-3′ 3′-r(AUGUC***A***GAUACA)-5′	53.2	+0.6
11	ON1 ON10	5′-r(UACAGUCUAUGU)-3′ 3′-r(AUGUCA***G***AUACA)-5′	53.1	+0.5
12	ON7 ON9	5′-r(UACAG***U***CUAUGU)-3′ 3′-r(AUGUC***A***GAUACA)-5′	54.2	+1.6
13	ON8 ON10	5′-r(UACAGU***C***UAUGU)-3′ 3′-r(AUGUCA***G***AUACA)-5′	55.3	+2.7

[a]Italics indicate 2′-F modification. Uppercase, bold, and red letters indicate TNA. [b]T_m values were obtained from the maxima of the first derivatives of the melting curves (A_{260} vs temperature) recorded in 1 × PBS buffer (pH 7.4) using 2.0 μM concentrations of each strand. [c]ΔT_m is the difference in melting temperature between the modified duplex and the reference RNA duplex 5′-r(UACAGUCUAUGU):3′-r(AUGUCAGAUACA), which had a T_m of 52.6 °C.

TNA are potent and have low toxicity when assayed in cultured mammalian cells and animal models.[40] Here, we report a systematic evaluation of siRNAs modified with TNA, demonstrating that site-specific modification with TNA can increase the potency, duration of action, and safety of therapeutics that act through the RNAi pathway.

RESULTS AND DISCUSSION

Monomer and Oligonucleotide Synthesis. The A, G, and T phosphoramidite building blocks of TNA (Figure 2) were synthesized based on the originally reported TNA synthesis protocol established by Eschenmoser and co-workers,[41,42] but optimized for scalability. The 5-methyl-C-TNA building block was synthesized by conversion of T-TNA via its triazole derivative with benzoyl protection (Scheme 1). The O6-DPC

https://doi.org/10.1021/jacs.3c04744
J. Am. Chem. Soc. XXXX, XXX, XXX−XXX

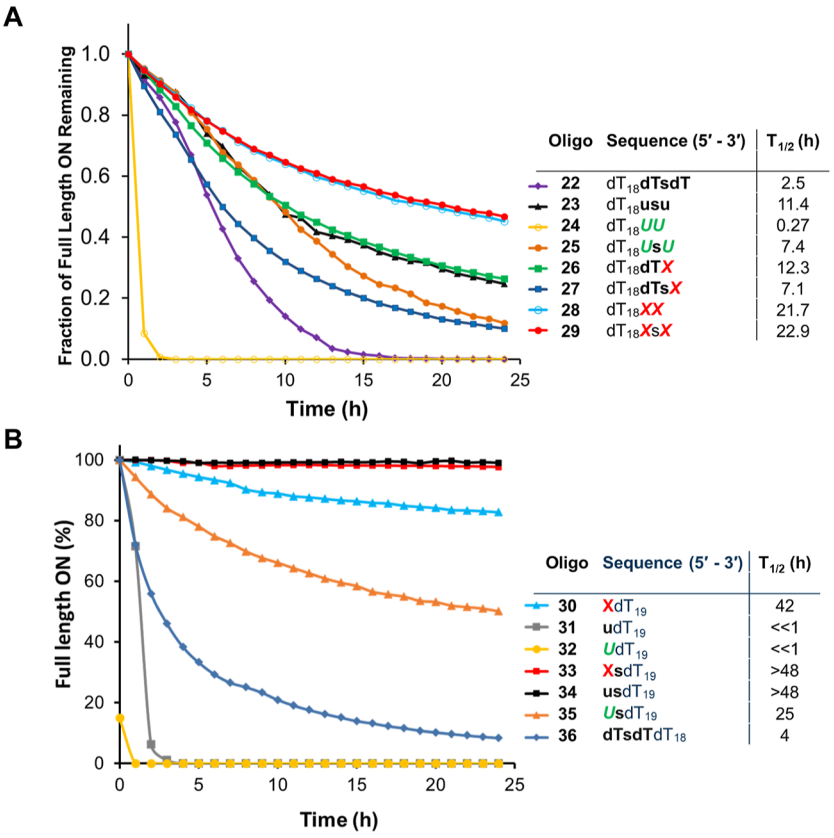

Figure 3. TNA protects an oligonucleotide from exonuclease digestion. (A) Percent full-length dT_{20}-mers modified at the 3′ end with T-TNA (X), 2′-*O*Me U (**u**), or 2′-F U (*U*) over time in the presence of SVPD. The **s** indicates a PS linkage. (B) Percent full-length dT_{20}-mers modified at the 5′ end with T-TNA (X), 2′-*O*Me U (**u**), or 2′-F U (*U*) over time in the presence of phosphodiesterase II. The **s** indicates a PS linkage.

group was used to favor glycosylation at the N-9 guanine position. This group remained on the molecule as its removal would reduce the overall yield of the synthesis. The details of the monomer building block synthesis are provided in the Supporting Information. The TNA-containing oligonucleotides were synthesized using solid-phase standard P(III) oligonucleotide chemistry on an automated RNA synthesizer with extended times (15 min) in the steps of phosphoramidite coupling and deblocking of the 5′-dimethoxytrityl group for TNA residues with 3% trichloroacetic acid (TCA). After cleavage from the solid support and standard deprotection,[12] the crude oligonucleotides were purified by reverse-phase HPLC and characterized by LC−MS analysis (Table S1, Figure S1).

Thermodynamic Stabilities of Duplexes That Contain TNA Monomers. The thermal melting temperatures (T_ms) of 12-mer RNA or DNA duplexes containing either a single TNA residue or one TNA−TNA base pair in an otherwise natural sequence were determined; 2′-F-modified duplexes were evaluated for comparison (Table 1 and Table S2). The modified residues were at position 6 or 7 from the 5′ end of one strand. The differences in the observed T_m values between the modified duplex and the RNA or DNA duplex control were calculated to evaluate the effect of the modification on the thermal stability. A single incorporation of TNA destabilized an otherwise all RNA duplex by ∼5 °C relative to the control RNA duplex with ΔT_m values ranging from −4.5 to −5.5 °C depending on the identity of the base. A TNA−TNA base pair in the context of an RNA duplex was more destabilizing than a single TNA with a T_m reduction of 9.5 °C for a T:A TNA base pair and 11.0 °C for a C:G base pair. In contrast, the 2′-F-modification slightly increased the stability of an RNA duplex by 0.5 to 1.7 °C. Similarly, incorporation of a 2′-F base pair moderately enhanced RNA duplex stability by 1.6 to 2.7 °C. Incorporation of TNA had less effect on DNA duplex thermal stability than on RNA duplex stability with ΔT_m values ranging from −2.3 to +1.6 °C relative to the DNA duplex control. A TNA base pair moderately destabilized the otherwise DNA duplex by about 2.5 °C. In DNA duplexes, the 2′-F modification resulted in stabilities comparable to or, in the case of 2′-F U, slightly less than the control.

Exonuclease-Mediated Degradation of Oligonucleotides with TNA Modifications. To assess the impact of a TNA modification on exonuclease-mediated degradation of oligonucleotides, T-TNA was incorporated at either the 3′ or 5′ end of a poly(T) oligodeoxynucleotide. The TNA was linked through a phosphodiester linkage (PO) or a phosphorothioate linkage (PS). The oligonucleotides were treated with 3′- or 5′-specific exonucleases, and time courses of the degradation of the full-length oligonucleotides were monitored using ion-exchange HPLC (Figure 3A and Table S3). When a single TNA was incorporated at 3′ terminus with a PO linkage (**ON26**), the half-life of the oligonucleotide in the presence of the 3′-specific exonuclease, snake venom phosphodiesterase (SVPD), was extended by about 5-fold when compared to the control with a single PS linkage at 3′ terminus (**ON22**). The stability of **ON26** was comparable to that of the oligonucleotide that terminates with two 2′-*O*Me residues with a PS linkage (**ON23**). The stability that results from a TNA incorporation is most likely due to the unique internucleotide linkage pattern of TNA through its secondary hydroxyl group at the 3′ position of the

https://doi.org/10.1021/jacs.3c04744
J. Am. Chem. Soc. XXXX, XXX, XXX−XXX

Table 2. Sequences of TNA-Modified siRNAs Targeting *Ttr* and Silencing Activities in Cell Culture

siRNA No.	sequence (5′-3′)	Strand ID[b]	Position of TNA	IC_{50} (nM)[c]
parent **si-0**	*A*●a●*CaGuGuUCUuGcUcUaUaA*(L) u●*U*●a*UaGaGcAagaAcAcUgUu*●u●u	S0 AS0		0.064
si-2	*A*●**A**●*CaGuGuUCUuGcUcUaUaA*(L) u●*U*●a*UaGaGcAagaAcAcUgUu*●u●u	S2 AS0	S2	0.110
si-9	*A*●a●*CaGuGu***T***CUuGcUcUaUaA*(L) u●*U*●a*UaGaGcAagaAcAcUgUu*●u●u	S9 AS0	S9	0.079
si-12	*A*●a●*CaGuGuUCU***T***GcUcUaUaA*(L) u●*U*●a*UaGaGcAagaAcAcUgUu*●u●u	S12 AS0	S12	0.075
si-17	*A*●a●*CaGuGuUCUuGcUc***T***aUaA*(L) u●*U*●a*UaGaGcAagaAcAcUgUu*●u●u	S17 AS0	S17	0.063
si-21	*A*●a●*CaGuGuUCUuGcUcUaUa***A***(L) u●*U*●a*UaGaGcAagaAcAcUgUu*●u●u	S21 AS0	S21	0.021
si-22	*A*●a●*CaGuGuUCUuGcUcUaUaA*(L) **T**●*U*●a*UaGaGcAagaAcAcUgUu*●u●u	S0 AS1	AS1	0.085
si-23	*A*●a●*CaGuGuUCUuGcUcUaUaA*(L) u●**T**●a*UaGaGcAagaAcAcUgUu*●u●u	S0 AS2	AS2	1.605
si-24	*A*●a●*CaGuGuUCUuGcUcUaUaA*(L) u●*U*●**A***UaGaGcAagaAcAcUgUu*●u●u	S0 AS3	AS3	0.047
si-25	*A*●a●*CaGuGuUCUuGcUcUaUaA*(L) u●*U*●a**T***aGaGcAagaAcAcUgUu*●u●u	S0 AS4	AS4	0.082
si-26	*A*●a●*CaGuGuUCUuGcUcUaUaA*(L) u●*U*●a*U***A***GaGcAagaAcAcUgUu*●u●u	S0 AS5	AS5	0.036
si-27	*A*●a●*CaGuGuUCUuGcUcUaUaA*(L) u●*U*●a*Ua***G***aGcAagaAcAcUgUu*●u●u	S0 AS6	AS6	0.068
si-28	*A*●a●*CaGuGuUCUuGcUcUaUaA*(L) u●*U*●a*UaG***A***GcAagaAcAcUgUu*●u●u	S0 AS7	AS7	0.047
si-29	*A*●a●*CaGuGuUCUuGcUcUaUaA*(L) u●*U*●a*UaG***G***cAagaAcAcUgUu*●u●u	S0 AS8	AS8	0.062
si-31	*A*●a●*CaGuGuUCUuGcUcUaUaA*(L) u●*U*●a*UaGaGc***A***agaAcAcUgUu*●u●u	S0 AS10	AS10	0.046
si-34	*A*●a●*CaGuGuUCUuGcUcUaUaA*(L) u●*U*●a*UaGaGcAag***A***AcAcUgUu*●u●u	S0 AS13	AS13	0.037
si-41	*A*●a●*CaGuGuUCUuGcUcUaUaA*(L) u●*U*●a*UaGaGcAagaAcAcUg***T***u●u●u	S0 AS20	AS20	0.076
si-46	*A*●**A**●*CaGuGuUCUuGcUcUaUaA*(L) u●*U*●a*UaGaGcAagaAcAcUg***T***u●u●u	S2 AS20	AS20	0.069
si-53	*A*●a●*CaGuGu***T***CUuGcUcUaUaA*(L) u●*U*●a*UaGaGcAag***A***AcAcUgUu*●u●u	S9 AS13	S9 AS13	0.060
si-56	*A*●a●*CaGuGuUCU***T***GcUcUaUaA*(L) u●*U*●a*UaGaGc***A***agaAcAcUgUu*●u●u	S12 AS10	S12 AS10	0.043
si-61	*A*●a●*CaGuGuUCUuGcUc***T***aUaA*(L) u●*U*●a*U***A***GaGcAagaAcAcUgUu*●u●u	S17 AS5	S17 AS5	0.028

[a]Italicized, uppercase letters indicate 2′-F. Lowercase letters indicate 2′-*O*Me. Uppercase, bold, and red letters represent TNA modifications. (L) represents the GalNAc ligand. PS linkages are indicated by the "●" symbol. [b]See Table S4 and Figure S2 for strand and duplex characterization data. S indicates the sense strand, and AS indicates the antisense strand. S0 and AS0 are parent sense and antisense strands that do not contain RNA. [c]IC_{50} values were determined in free-uptake conditions with doses from 100 to 3.57×10^{-4} nM final duplex concentration. *Ttr* mRNA was quantified by RT-PCR. *GAPDH* was quantified as the internal control. Data given are means of four independent experiments.

threose sugar. Interestingly, when the TNA was linked through a PS linkage (**ON27**), the stability against SVPD digestion was lower than that of the oligonucleotide with a PO linkage (**ON26**). A similar effect of the linkage was observed with the GNA modification.[13,27]

The oligonucleotide with two TNA residues connected by a PO linkage at 3′ terminus (**ON28**) had a half-life of 21.7 h, which is significantly more stable than the oligonucleotide modified with a single TNA (**ON26**). In this case, the oligonucleotide with a PS linkage (**ON29**) was more stable than that with the PO linkage, although the increase in nuclease resistance was marginal. The oligonucleotide with two TNAs linked through a PO had a half-life considerably longer than those of oligonucleotides modified with two 2′-*O*Me residues connected with a PS linkage (**ON23**), with two 2′-F modifications and a PO linkage (**ON24**), or with two 2′-F modifications and a PS linkage (**ON25**) by 2-, 80-, and 3-fold, respectively.

The effect of the TNA modification on resistance toward the 5′-exonuclease, phosphodiesterase II, was also noteworthy (Figure 3B, Table S3). The oligonucleotide with a single incorporation of TNA with a PO linkage at 5′ terminus (**ON30**) was 10-fold more resistant against degradation than the control with single PS linkage (**ON36**); **ON30** was only 17% degraded after 24 h. In contrast, when 2′-*O*Me (**ON31**) or 2′-F (**ON32**) was placed at the 5′ end with PO linkage, the oligonucleotides were rapidly degraded. TNA in combination with a PS linkage (**ON33**) was almost completely resistant to degradation by the 5′-exonuclease, with negligible degradation in 24 h. Thus, in contrast to the effect at the 3′ terminus, the PS linkage was beneficial at the 5′ terminus. The oligonucleotide with a 2′-*O*Me with a PS linkage (**ON34**) was as stable as **ON33**, but the 2′-F/PS-modified oligonucleotide (**ON35**) was very susceptible to the exonuclease-mediated degradation. These results that demonstrate the resistance of TNA-modified oligonucleotides

https://doi.org/10.1021/jacs.3c04744
J. Am. Chem. Soc. XXXX, XXX, XXX−XXX

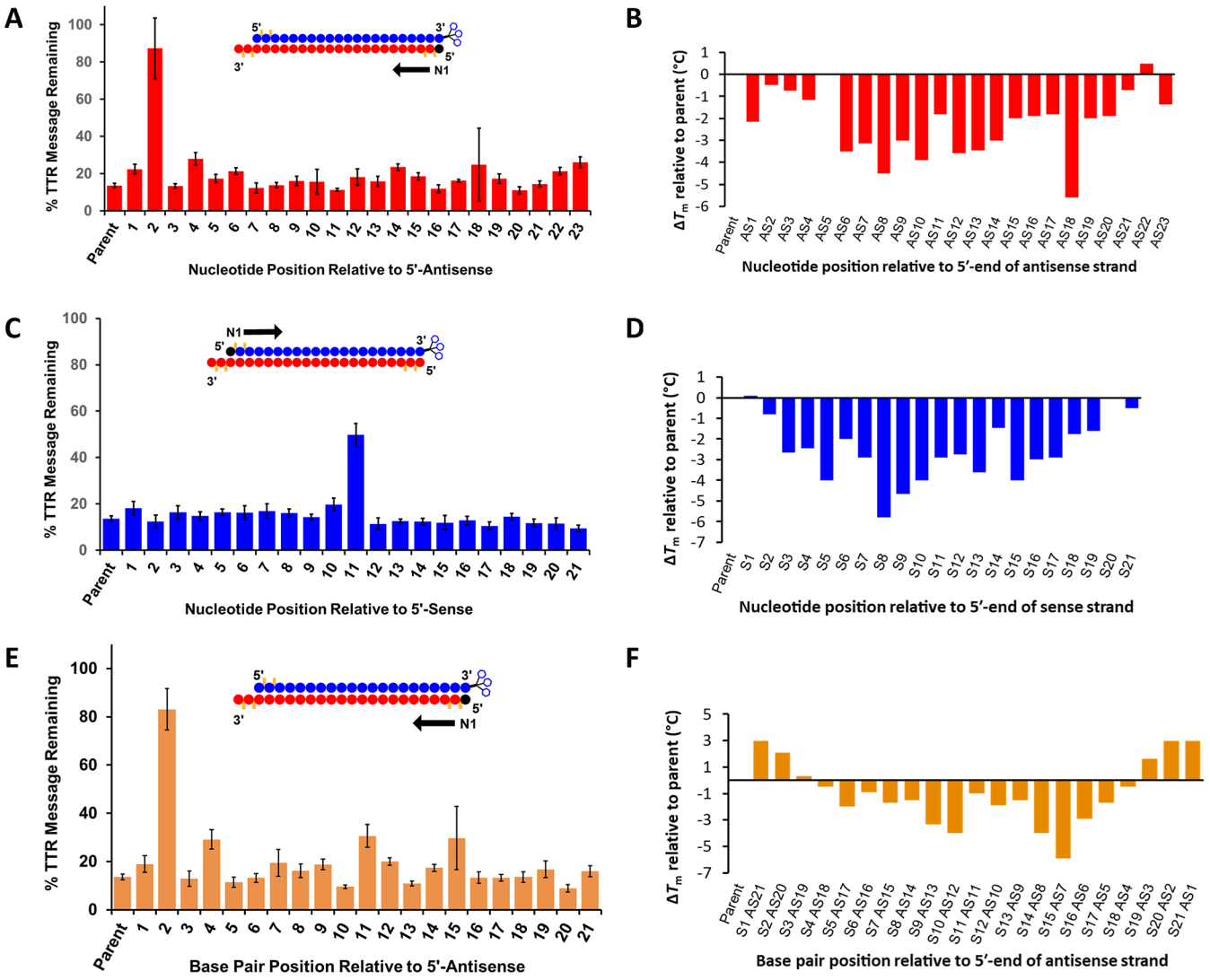

Figure 4. Single TNA modifications at most positions have little effect on the in vitro efficacy but decrease the siRNA duplex thermal stability. (A) Percent *Ttr* mRNA remaining when cells were treated with siRNA with TNA at the indicated position relative to the 5′ end of the antisense strand. N1 refers to position 1 in the antisense strand (red), and the arrow represents the direction of TNA placement. (B) Change in T_m relative to the parent siRNA duplex as a function of TNA modification in the antisense strand. (C) Percent *Ttr* mRNA remaining when cells were treated with siRNA with TNA at the indicated position relative to the 5′ end of the sense strand. N1 refers to position 1 of the sense strand (blue), and the arrow represents the direction of TNA placement. (D) Change in T_m relative to the parent siRNA duplex as a function of TNA modification in the sense strand. (E) Percent *Ttr* mRNA remaining when cells were treated with siRNA with TNA base pairs at the indicated position relative to the 5′ end of the antisense strand. (F) Change in T_m relative to the parent siRNA duplex upon incorporation of a TNA base pair. For analysis of in vitro silencing, levels of *Ttr* mRNA were quantified using RT-qPCR after incubation of primary mouse hepatocytes with 1 nM siRNA for 48 h. Amounts were normalized to *Ttr* mRNA in cells treated with a non-targeting siRNA. All data points are the averages ± standard deviation of four measurements. ΔT_m is the difference in melting temperature between the modified duplex and the reference siRNA duplex **si-0** had a T_m of 79.0 °C.

to nuclease-mediated degradation are consistent with the previously reported studies.[26]

In Vitro Gene Silencing Activity of TNA-Containing siRNA Duplexes. We evaluated the impact of TNA modifications on RNAi-mediated gene silencing activity of an siRNA duplex targeting the mouse *Ttr* mRNA. The parent siRNA duplex was a 21-mer duplex with a two-nucleotide overhang at the 3′ end of the antisense strand (Figure 1A) that has well-characterized gene silencing activity in vitro and in vivo.[13,43−46] Sense and antisense strands of the parent siRNA were fully modified with 2′-*O*Me and 2′-F. Both termini of the antisense strand and the 5′ end of the sense strand had PS linkages, and the 3′ end of the sense strand was conjugated with a triantenary GalNAc ligand through a hydroxyprolinol linker.

To systematically examine the positional effect of the TNA modification on the gene silencing activity, each nucleotide in sense and antisense strands was individually replaced with its TNA nucleotide counterpart. Similarly, each of the base pairs was substituted with the corresponding TNA−TNA base pair. siRNA duplex sequences are given in Table 2. By analyses of thermal melting, we confirmed that each siRNA duplex containing a TNA modification or a TNA base pair was stable; the differences in T_m between the TNA-containing siRNA and the parent siRNA ranged from +3 to −6.0 °C (Figure 4BD,F).

The potency of the *Ttr* gene silencing by each siRNA duplex was initially evaluated at two doses: 1 and 100 nM. *Ttr* mRNA was quantified using real-time qPCR at 48 h after addition of the siRNA to primary mouse hepatocytes under free-uptake

https://doi.org/10.1021/jacs.3c04744
J. Am. Chem. Soc. XXXX, XXX, XXX−XXX

conditions (i.e., without transfection reagent). For siRNAs with single TNA residues (Figure 4A,C), TNA was not tolerated at position 2 of the antisense strand or at position 11 of the sense strand. This is consistent with previously reported research that has demonstrated that chemical modifications other than 2′-F, 2′-H, and 2′-OH are not tolerated at these positions.[8] Potency was comparable to or slightly worse than that of the parent siRNA when TNA was incorporated at other positions on the antisense strand and was comparable to the parent when TNA was incorporated at other positions on the sense strand. It is noteworthy that modification of positions 7 and 8 in the seed region of the antisense strand with TNA did not decrease potency relative to the parent siRNA. When a TNA base pair was incorporated into the *Ttr*-targeted siRNA, impacts of position were similar to that observed with single TNA modifications (Figure 4E). The activity was considerably impaired due to modification at position 2 of the antisense strand, and TNA base pairs at positions 4, 11, and 15 of the antisense strand also reduced the activity slightly. TNA base pairs were well tolerated at positions 5−10 of the antisense strand, which is within the seed region.

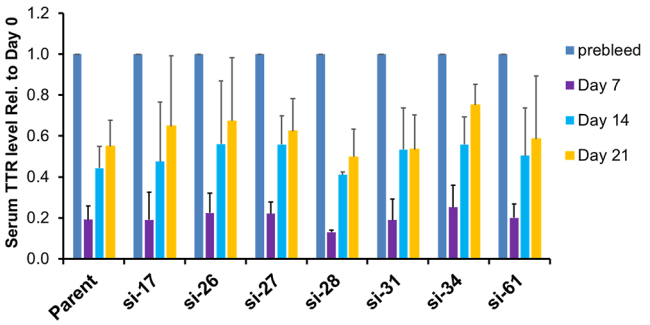

Figure 5. TNA modifications do not impair in vivo efficacy in mice. Serum TTR levels in mice treated with indicated the parent or TNA-modified siRNAs. Animals received a single subcutaneous dose of 1.0 mg/kg siRNA (n = 3 per group). Immediately before treatment (pre-bleed) and at indicated times post-dosing of animals, TTR was measured in serum using a sandwich ELISA utilizing an HRP-conjugate antibody and 3,3′,5,5′-tetramethylbenzidine for readout at 450 nm. All samples were analyzed in duplicate, and each data point is the average ± standard deviation normalized to pre-dose levels in an individual animal.

To quantitatively assess the impact of TNA modifications on the gene-silencing activity, we determined the half-maximal inhibitory concentration (IC_{50}) values of siRNA duplexes by analyses of percent *Ttr* mRNA at 48 h after treatment of mouse primary hepatocytes with a range of concentrations of siRNA under free-uptake conditions (Figure S4 and Table 2). TNA was not, as expected, tolerated at position 2 on the antisense strand. **si-23** had an IC_{50} of 1.6 nM, a 25-fold loss of potency relative to the parent, which had an IC_{50} of 0.064 nM. Single incorporations at other positions were well tolerated. For example, when TNA was incorporated at position 5 in the seed region of the antisense strand (**si-26**), the IC_{50} was 0.036 nM. IC_{50} values of siRNAs modified at other positions in the seed region ranged from 0.036 to 0.082 nM. In the sense strand, only modification at position 11 was not tolerated. For example, when a TNA was placed at position 17 (across from position 5 in the seed region of the antisense strand) in the sense strand (**si-17**), the IC_{50} was 0.063 nM, equivalent to the parent. In most cases, siRNAs with TNA base pairs had potency similar to or better than that of the parent. For example, the siRNA with TNA modifications at position 5 of the antisense strand and position 17 of the sense strand (**si-61**) had an IC_{50} of 0.028 nM. These data suggest that TNA is well tolerated in most positions in an siRNA.

To determine whether there was a correlation between thermodynamic stabilities of the duplexes containing TNA monomers and in vitro silencing activity, we plotted the IC_{50} values versus the difference in T_m between the TNA-modified siRNA and the parent. There was no correlation between the siRNA duplex binding affinity and silencing efficiency. This indicates that siRNA duplex stability is not a critical factor in RISC activity, except for the effect on the previously described strand-asymmetry-mediated displacement of the sense strand during the loading of the antisense strand into RISC.[47]

In Vivo Efficacy of TNA-Modified siRNA Targeting *Ttr*. We next evaluated several TNA-modified siRNAs in mice. Mice were given a single subcutaneous dose of 1.0 mg/kg of the siRNA, and TTR protein was monitored in serum over a period of 21 days (Figure 5 and Table 3). At day 7, the parent siRNA without TNA modification (**si-0**) suppressed levels of

Table 3. Evaluation of Gene Silencing Induced by siRNAs Modified with TNA in Mice

siRNA ID	Sequences (5′-3′)[a]	Strand ID[b]	TNA
si-0	*A*●a●CaGuGuUCUuGcUcUaUa*A*(L)	S0	
	u●*U*●a*U*a*G*a*G*c*A*aga*A*c*A*c*U*g*U*u●u●u	AS0	
si-17	*A*●a●CaGuGuUCUuGcU**c**Ta*U*a*A*(L)	S17	N17 of S
	u●*U*●a*U*a*G*a*G*c*A*aga*A*c*A*c*U*g*U*u●u●u	AS0	
si-26	*A*●a●CaGuGuUCUuGcUcUa*U*a*A*(L)	S0	N5 of AS
	u●*U*●a**U**A*G*a*G*c*A*aga*A*c*A*c*U*g*U*u●u●u	AS5	
si-27	*A*●a●CaGuGuUCUuGcUcUa*U*a*A*(L)	S0	N6 of AS
	u●*U*●a*U*a**G**a*G*c*A*aga*A*c*A*c*U*g*U*u●u●u	AS6	
si-28	*A*●a●CaGuGuUCUuGcUcUa*U*a*A*(L)	S0	N7 of AS
	u●*U*●a*U*a*G***A***G*c*A*aga*A*c*A*c*U*g*U*u●u●u	AS7	
si-31	*A*●a●CaGuGuUCUuGcUcUa*U*a*A*(L)	S0	N10 of AS
	u●*U*●a*U*a*G*a*G*c**A***A*aga*A*c*A*c*U*g*U*u●u●u	AS10	
si-34	*A*●a●CaGuGuUCUuGcUcUa*U*a*A*(L)	S0	N13 of AS
	u●*U*●a*U*a*G*a*G*c*A*ag**A***A*c*A*c*U*g*U*u●u●u	AS13	
si-61	*A*●a●CaGuGuUCUuGcU**c**Ta*U*a*A*(L)	S17	N17 of S
	u●*U*●a**U**A*G*a*G*c*A*aga*A*c*A*c*U*g*U*u●u●u	AS5	N5 of AS

[a]Italicized uppercase letters indicate 2′-F. Lowercase indicates 2′-*O*Me. Uppercase, bold, red letters represent TNA modifications. ● indicates phosphorothioate. (L) indicates trivalent GalNAc. [b]See Table S4 for strand characterization data. S indicates the sense strand, and AS indicates the antisense strand. S0 and AS0 are parent sense and antisense strands that do not contain TNA.

https://doi.org/10.1021/jacs.3c04744
J. Am. Chem. Soc. XXXX, XXX, XXX−XXX

Table 4. Sequences of siRNAs with the Antisense Strand 5′-Terminally Modified with TNA with or without Phosphorylation

siRNA ID	Sequences (5′-3′)[a]	Strand ID[b]
si-66	a●a●*CaGuGuUCUuGcUcUaUaA*(L)	S22
	T*U*●a*UaGaGcAagaAcAcUgUu*●u●u	AS24
si-67	a●a●*CaGuGuUCUuGcUcUaUaA*(L)	S22
	PT*U*●a*UaGaGcAagaAcAcUgUu*●u●u	AS25
si-68	a●a●*CaGuGuUCUuGcUcUaUaA*(L)	S22
	T●*U*●a*UaGaGcAagaAcAcUgUu*●u●u	AS26
si-69	a●a●*CaGuGuUCUuGcUcUaUaA*(L)	S22
	PT●*U*●a*UaGaGcAagaAcAcUgUu*●u●u	AS27
si-70 (Control)	a●a●*CaGuGuUCUuGcUcUaUaA*(L)	S22
	Pu*U*●a*UaGaGcAagaAcAcUgUu*●u●u	AS28
si-71 (Control)	a●a●*CaGuGuUCUuGcUcUaUaA*(L)	S22
	Pu●*U*●a*UaGaGcAagaAcAcUgUu*●u●u	AS29
si-77 (Control)	a●a●*CaGuGuUCUuGcUcUaUaA*(L)	S22
	u●*U*●a*UaGaGcAagaAcAcUgUu*●u●u	AS0
si-78 (Control)	a●a●*CaGuGuUCUuGcUcUaUaA*(L)	S22
	u*U*●a*UaGaGcAagaAcAcUgUu*●u●u	AS35

[a]Italicized uppercase letters indicate 2′-F. Lowercase letters indicate 2′-*O*Me. Uppercase, bold, red letters indicate T-TNA. **P** indicates 5′-phosphate; ● indicates PS; (L) indicates trivalent GalNAc ligand. [b]See Table S4 for strand characterization data. S indicates the sense strand, and AS indicates the antisense strand. S0 and AS0 are parent sense and antisense strands that do not contain RNA.

circulating TTR protein by 81% compared to pre-dose levels, and the levels had returned to normal by day 21. The siRNA with TNA at position 7 of the antisense strand (**si-28**) had better efficacy than that of the parent through day 21. Placement of TNA in the seed region of the antisense strand at position 5 (**si-26**), position 6 (**si-27**), or position 10 (**si-31**) resulted in activity comparable to that of the parent. Modification at position 13 of the antisense strand (**si-34**) caused a slight decrease in activity. siRNAs with a TNA modification in the sense strand at position 17 (**si-17**) or a TNA base pair in the seed region (**si-61**) also had activity comparable to that of the parent.

In Vitro and In Vivo Efficacy of siRNAs Targeting *Ttr* with TNA in Position 1 of the Antisense Strand. The phosphorylation of the 5′ terminus of the antisense strand is essential for siRNA activity. Thus, we evaluated the impact of TNA at position 1 of the antisense strand with or without a 5′ phosphate (Table 4). Regardless of whether a phosphate group was pre-installed at the 5′ terminus of the TNA-modified antisense strand, the silencing activities under transfection or free-uptake conditions in primary mouse hepatocytes were comparable to that of the siRNA with a terminal 5′-phosphorylated 2′-*O*Me U (Figure 6A,B). We also evaluated the set of siRNAs with and without a 5′ phosphate in mice (Figure 6C). Mice treated with a single dose of 1.0 mg/kg and

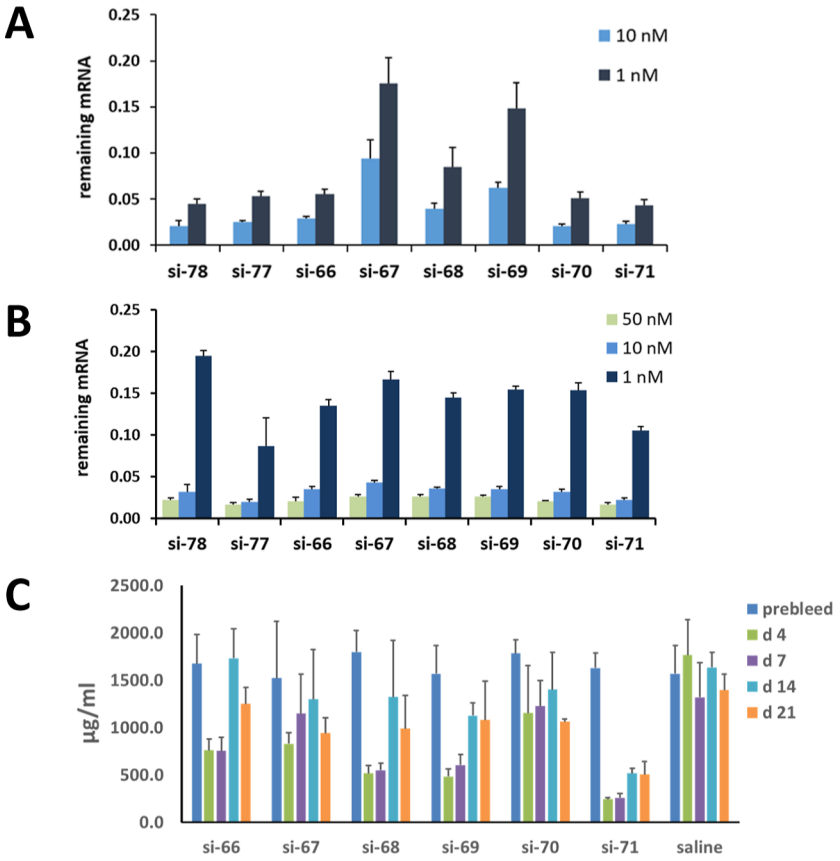

Figure 6. Phosphorylation of the TNA-modified 5′ terminus of the antisense strand is not necessary for activity. (A,B) *Ttr* mRNA remaining after 24 h in primary mouse hepatocytes treated with siRNAs modified at the 5′ terminus of the antisense strand with TNA under (A) transfection conditions and (B) free-uptake conditions. Amounts were normalized to *Ttr* mRNA in cells treated with a non-targeting siRNA. Data are means ± standard deviation of four experiments. (C) Serum TTR levels in mice treated with indicated TNA-modified siRNA duplexes. Animals received a single dose of 1.0 mg/kg siRNA (n = 3 per group). Prior to treatment (pre-bleed) or at the indicated time post-dosing, TTR was measured in serum using a sandwich ELISA assay utilizing an HRP-conjugate antibody and 3,3′,5,5′-tetramethylbenzidine for readout at 450 nm. All samples were measured in duplicate, and each data point is the average ± standard deviation normalized to the pre-dose level in individual animals.

https://doi.org/10.1021/jacs.3c04744
J. Am. Chem. Soc. XXXX, XXX, XXX−XXX

Table 5. Sequences Used for Evaluation of Off-Target Effects of siRNAs Modified with TNA in Mice

siRNA ID	Sequences (5′-3′)[a]	Strand ID[b]	Position of TNA
si-72	a●a●caguGuUCUugcucuauaa(L)	S23	
	u●U●auaGagcaagaAcAcuguu●u●u	AS30	
si-73	a●a●caguGuUCUugcucuauaa(L)	S23	N5 of AS
	u●U●auAGagcaagaAcAcuguu●u●u	AS31	
si-74	a●a●caguGuUCUugcucuauaa(L)	S23	N6 of AS
	u●U●auaGagcaagaAcAcuguu●u●u	AS32	
si-75	a●a●caguGuUCUugcucuauaa(L)	S23	N7 of AS
	u●U●auaGAgcaagaAcAcuguu●u●u	AS33	
si-76	a●a●caguGuUCUugcucuauaa(L)	S23	N8 of AS
	u●U●auaGaGcaagaAcAcuguu●u●u	AS34	

[a]Italicized uppercase letters indicate 2′-F. Lowercase letters indicate 2′-*O*Me. Uppercase, bold, red letters indicate TNA. ● indicates PS, and (L) indicates trivalent GalNAc. [b]See the Supporting Information for strand nomenclature. See Table S4 for strand characterization data. S indicates the sense strand, and AS indicates the antisense strand.

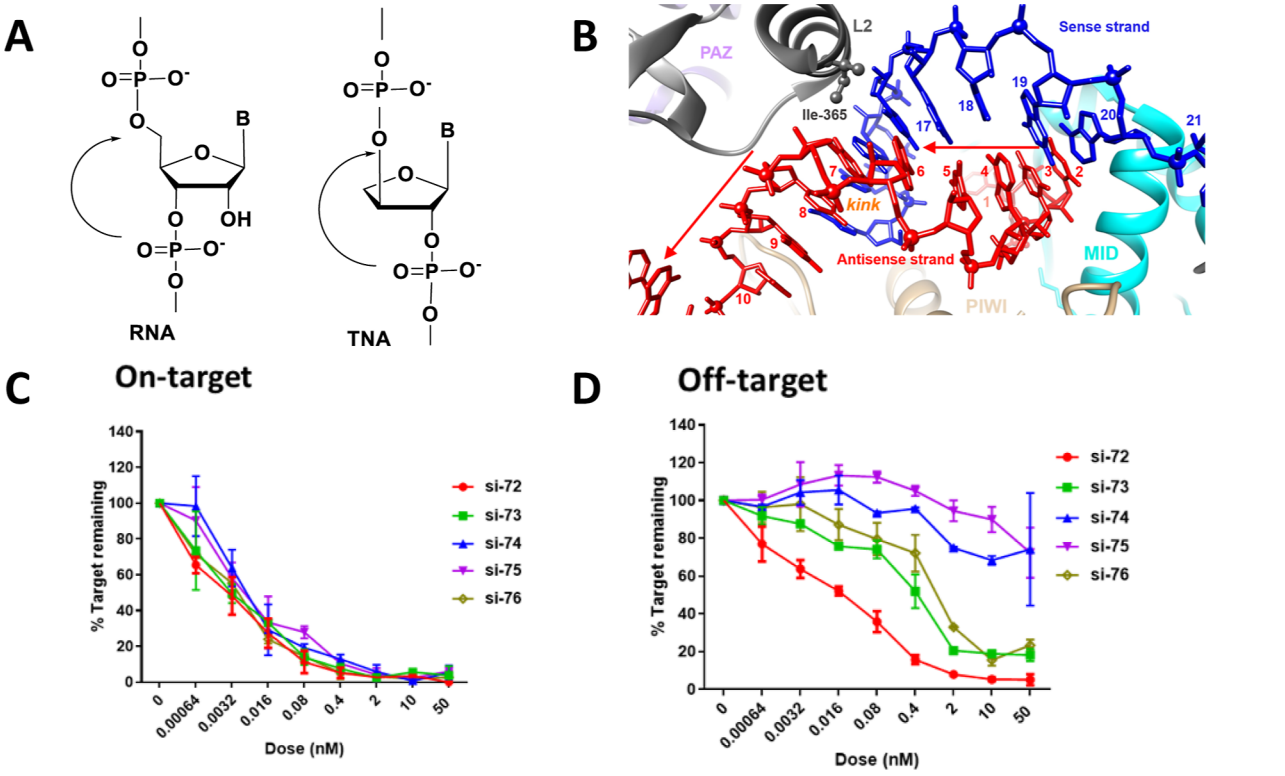

Figure 7. TNA in the seed region mitigates off-target activity. (A) Structure of RNA vs. TNA showing the shorter internucleotide distances. (B) View of the crystal structure of Ago2 bound to an RNA duplex (PDB ID 4W5T) kinked between positions 6 and 7 of the antisense strand ("kink"). Ago2 domains are highlighted and labeled, and the siRNA (antisense and sense) strands are colored in red and blue, respectively. Antisense strand residues 1−10 are numbered. Also shown is the side chain of isoleucine 365 in ball-and-stick mode; the color code for Ago2 domains (MID, PIWI, L2, PAZ) is the same as before. See also the modeling discussion below. (C) Percent target remaining as a function of siRNA concentration in the on-target dual-luciferase assay. (D) Percent target remaining as a function of siRNA concentration in the off-target dual-luciferase reporter assay. siRNAs were transfected into COS-7 cells at the indicated concentrations along with the reporter plasmid. *Renilla* and firefly luciferase activities were measured 48 h after transfection and plotted as the ratio at each concentration normalized to control samples not treated with siRNA from three independent experiments.

serum levels of TTR were followed for 21 days. The activity of **si-71**, the compound with a 5′ phosphate and a terminal PS linkage, was more potent and durable than that of the 5′ phosphorylated parent with a PO linkage (**si-70**). The four siRNAs with 5′-terminal TNA were more active than **si-70** but less active than **si-71**. These data indicate that TNA provides metabolic stability. Furthermore, our finding that the siRNA with a 5′-terminal TNA but without a 5′ phosphate (**si-68**) is active suggests that the cellular kinase machinery phosphorylates the 3′ hydroxyl of the TNA residue at the 5′ end of the antisense strand. The potency was also independent of whether the linkage between position 1 and 2 of the antisense strand was PO or PS: The activity and duration of action of **si-69**, which has 5′-terminal TNA linked through PO and a 5′ phosphate, was only slightly compromised compared to **si-71**.

TNA Modification Mitigates Off-Target Effects. siRNAs can induce off-target effects due to miRNA-type interactions with non-targeted mRNAs that occur through the seed region of the antisense strand. As TNA has a short internucleotide length resulting in thermodynamically less stable duplexes, we reasoned that it should reduce off-target effects as was shown previously for the destabilizing GNA modification.[48] To assess

https://doi.org/10.1021/jacs.3c04744
J. Am. Chem. Soc. XXXX, XXX, XXX−XXX

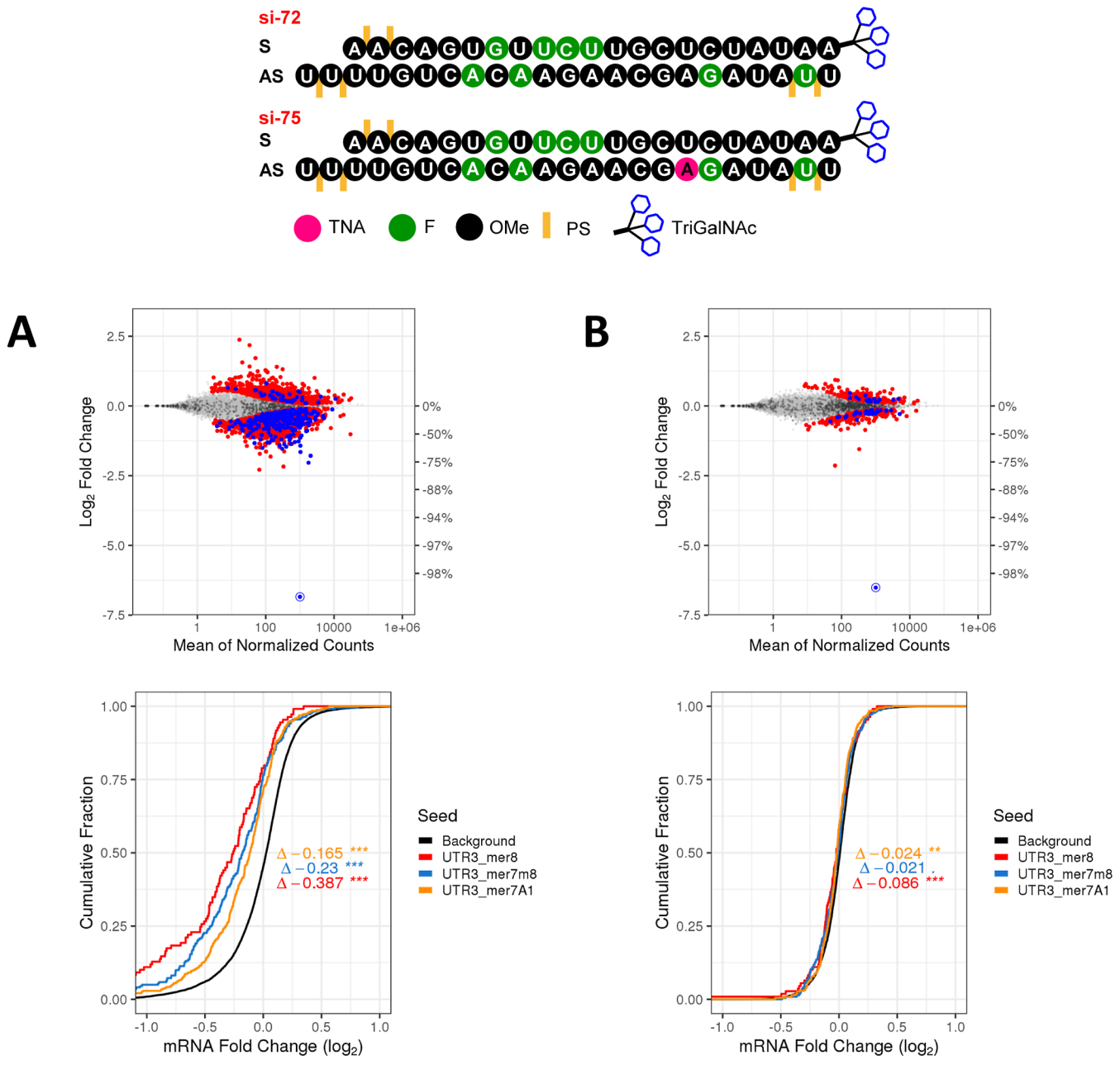

Figure 8. TNA mitigates off-target activity as shown by transcriptome analysis. Primary rat hepatocytes were treated with 50 nM of (A) parent siRNA **si-72** or (B) TNA-modified **si-75**. After 48 h, total RNA was isolated and subjected to RNA-seq analysis. These experiments were conducted using four wells/replicates per condition in primary rat hepatocytes. Upper: Plots of $\log_2$ fold change vs abundance (average counts) of individual genes. Dots represent individual transcripts. Gray dots represent genes not differentially expressed after siRNA treatment relative to the control; the blue and red dots represent differentially expressed genes (false discovery rate <0.05) with or without a canonical seed match,[49] respectively. On-target knockdown of *Ttr* is indicated by the circled dot. Lower: Cumulative distribution plots, which visualize the fraction of genes below a given $\log_2$ fold change, show the magnitude of dysregulation for gene sets in different canonical 3′-UTR seed match categories relative to the background set of genes lacking 3′-UTR seed matches in these categories (black).

how TNA incorporation into the seed region impacts on- and off-target activity, we utilized a previously described dual-luciferase assay.[14,45] The parent GalNAc-siRNA (**si-72**, Table 5) or versions containing TNA modifications at positions 5, 6, 7, or 8 in the antisense strand (**si-73**, **si-74**, **si-75**, and **si-76**, Table 5) were co-transfected into COS-7 cells along with the reporter plasmid for the expression of control firefly *luciferase* and *Renilla luciferase* containing either a single on-target siRNA binding site in the 3′-untranslated region (3′-UTR) or four tandem sites that are complementary to the siRNA antisense seed region (positions 5−8) but not the rest of the antisense strand, in the 3′-UTR. The siRNAs with TNA modifications had on-target activity essentially equivalent to that of the parent siRNA as assessed using the reporter containing a single site fully matched to the antisense strand (Figure 7C,D). Importantly, TNA at position 5 or 8 partially mitigated off-target effects, and TNA at position 6 or 7 almost completely inhibited off-target activity (Figure 7C,D).

To further evaluate the impact of TNA on off-target activity, we performed an RNA-seq analysis to measure the extent of

https://doi.org/10.1021/jacs.3c04744
J. Am. Chem. Soc. XXXX, XXX, XXX−XXX

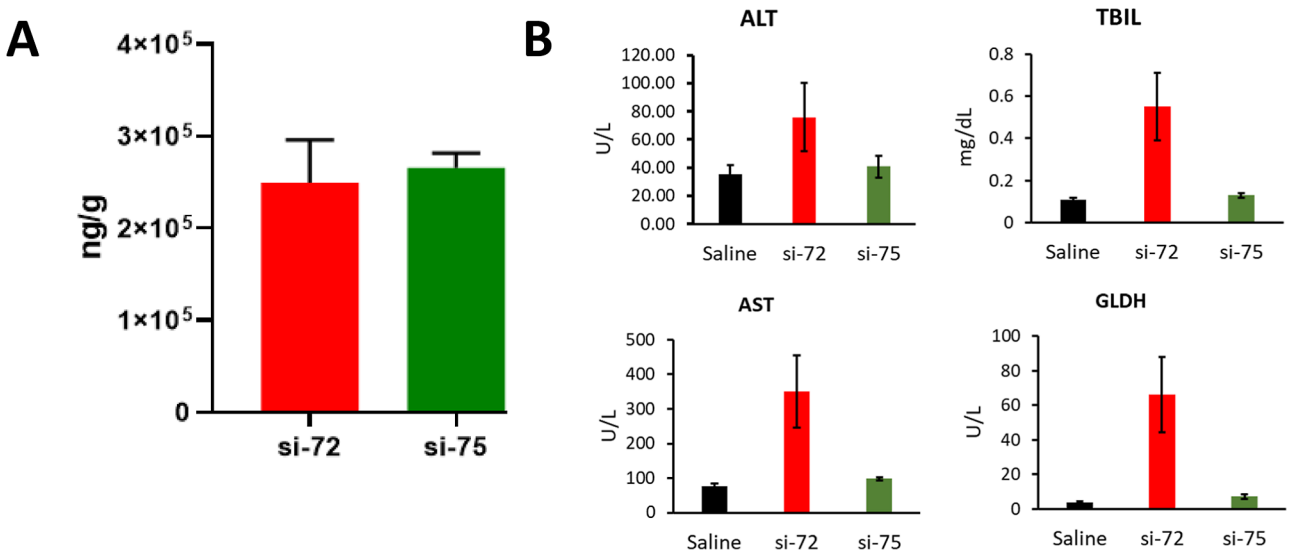

Figure 9. Seed TNA modification mitigates hepatotoxicity in rats. GalNAc-siRNAs **si-72** and **si-75** were administered subcutaneously to Sprague-Dawley rats ($n = 3$) at 30 mg/kg on days 1, 8, and 15. (A) Total drug levels in the liver at 24 h after the last dose. (B) Alanine aminotransferase (ALT), total bilirubin (TBIL), aspartate aminotransferase (AST), and glutamate dehydrogenase (GLDH) in serum at 24 h after the last dose. Means ± standard deviation of three animals per group.

transcriptional dysregulation in rat hepatocytes treated with siRNAs. Numerous transcripts were found to be dysregulated after 48 h of treatment with the parent siRNA, **si-72** (Figure 8A). Many of these transcripts contained a region complementary to the antisense seed region. Consistent with the off-target luciferase reporter data, incorporation of TNA at position 7 in the antisense strand (**si-75**) resulted in a significant reduction in transcriptional dysregulation compared to the parent (Figure 8B). Thus, TNA in the seed region can mitigate siRNA off-target activity.

We next evaluated the safety of TNA siRNA against the control at doses considerably higher than the pharmacologically effective dose in rats. Three weekly 30 mg/kg subcutaneous injections of **si-72** and **si-75** were administered. The total drug levels in the liver were the same (Figure 9A) for both compounds, but **si-72** led to elevated levels of liver injury markers at 24 h after the last dose, whereas **si-75** did not (Figure 9B). Sections processed from liver tissue collected at necropsy were stained with hematoxylin and eosin. Administration of **si-72** was associated with moderate single-cell necrosis and increased mitotic figures, mild to moderate hepatocellular vacuolation, minimal karyomegaly, hypertrophy, and hyperplasia of Kupffer cells, and biliary hyperplasia (Table S5). The TNA-containing **si-75** caused minimal single-cell necrosis and mitotic figures and mild hepatocellular vacuolation, and there was no microscopic evidence of karyomegaly or biliary hyperplasia (Table S5). The fact that a TNA residue in the seed region of the antisense strand mitigates hepatotoxicity likely results from reduced off-target silencing.

Structure of an RNA Octamer Containing T-TNA. The conformation of an RNA strand containing TNA had not been determined. To fill this void, we solved the crystal structure of an RNA duplex with a single TNA nucleotide in each strand. We performed crystallization trials with duplexes with several different sequences and obtained well-diffracting crystals for several. Diffraction data were phased with either 5-bromo-U or 5-bromo-C and revealed orientational disorder with both octamer and dodecamer crystals. For example, in the crystal form with space group (s.g.) $P3_221$ of the octamer of 5′-(Br5C)GAAU(T)CG-3′ (T-TNA indicated in red font), which diffracted to 1.07 Å resolution, the experimental electron density showed bromine positions that mapped to paired nucleotides. Moreover, there was a density for phosphate groups between adjacent duplexes. Both observations are indicative of strand slippage along the direction of the helical axis of infinitely stacked duplexes. Diffraction data to 1.3 Å resolution for a second crystal form of the same octamer could be indexed in s.g. *P*1 (*R*-merge 0.089, *R*-pim 0.029), *C*2 (*R*-merge 0.083, *R*-pim 0.019), *R*3 (*R*-merge 0.088, *R*-pim 0.017), as well as *R*32 (Table S6). In this crystal, octamers also exhibited multiple orientations, with bromine providing guidance with respect to the number and occupancy of sites and specific shifts of individual octamers (Figure 10A). Because of the particular symmetry of the crystal, the structure could be four slipped and partially superimposed octamer duplexes in s.g. *P*1, four slipped and partially superimposed dodecamer single strands in s.g. *C*2, four slipped and partially superimposed tetramer duplexes in s.g. *R*3, or four slipped and partially superimposed tetramer single strands in s.g. *R*32. We are not aware of another case of such an unusual disorder in an oligonucleotide crystal.

We performed refinement of data indexed in s.g. *C*2. The refined structure of a single dodecamer strand among the four slipped and superimposed dodecamers is depicted in Figure 10B. An image of the contents of the *C*2 unit cell is shown in Figure S5. The pucker of the T-TNA is C4′-*exo* (northeast conformer). This is the same pucker type that we previously observed by X-ray crystallography for TNA nucleotides incorporated into a B-form DNA[50] and into an A-form DNA duplex.[51] The same pucker was also adopted by TNA nucleotides in a self-complementary TNA duplex studied by solution NMR[52] and in crystal structures of TNA-modified DNA template-primer duplexes bound to an engineered TNA polymerase.[53] In contrast, isolated TNA pyrimidine and purine nucleotides trapped in crystal structures of an RNA hairpin or duplex constructs had either a C2′-*exo* (high-north) or C3′-*endo* (north) pucker.[54]

Structural Analysis of TNA in siRNA Using Molecular Modeling. To better understand the effects of TNA

https://doi.org/10.1021/jacs.3c04744
J. Am. Chem. Soc. XXXX, XXX, XXX−XXX

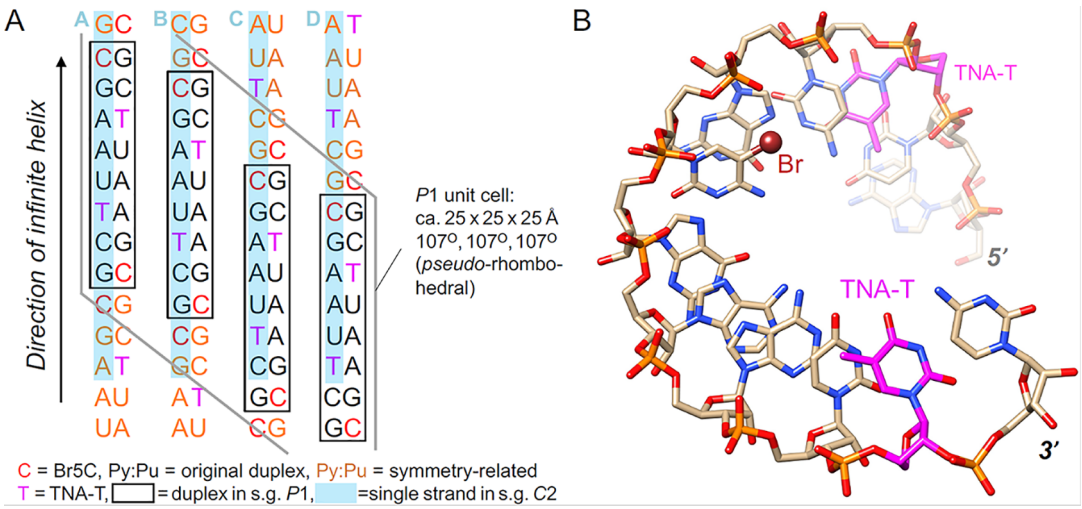

Figure 10. Crystal structure of TNA in a self-complementary RNA 8-mer reveals octamer duplexes in infinite stacks. (A) Illustration of the unit cell contents of the $[(Br5C)GAAU(\mathbf{T})CG]_2$ crystal in space groups *P*1 and *C*2 (sub-group of rhombohedral *R*32). The four slipped dodecamer strands in *C*2 are labeled A to D. (B) Structure of dodecamer C with TNA residues highlighted in magenta, and bromine shown as a maroon sphere.

modification on activity, we modeled siRNAs containing TNA residues in complex with Ago2. Models were built in the UCSF Chimera suite[55] using the crystal structure of the complex between Ago2 and miR-20a (PDB ID 4F3T), as reported previously.56 The TNA-T was taken from the crystal structure of the modified RNA octamer, and the methyl group was removed to yield U-TNA. The TNA-A residue was taken from the crystal structure of the TNA-modified A-form DNA decamer.[51] The manually built complexes with TNA-U at position 1, TNA-A at position 2, and TNA-A at position 3 were energy-minimized with Amber (ff14).[57] The results are shown in Figure 11.

In each case, the tetrose sugar of the TNA adopts the C4′-*exo* pucker. At position 1, where the ribose in the parent complex has a DNA-like (south) pucker, modification with TNA results in a distance that is approximately 1 Å shorter between the 5′ phosphate and the first bridging phosphate than when this is a ribose residue (Figure 11A). The tetrose and ribose sugars show little overlap, but the base is shifted slightly in the TNA-modified strand resulting in stacking with Y529. In addition, the tight turn between positions 1 and 2 observed in the complex of Ago2 with RNA is conserved in the strand modified with TNA, with only a slight shift of the position 2 phosphate; other residues have conformations and interactions with Ago2 that do not differ from those observed with the unmodified RNA. For the strand modified with TNA at position 2, a position at which only 2′-deoxyribose, ribose, or 2′-F moieties are tolerated,[8,10] the threose causes no steric problems; however, the structural framework of TNA results in a different orientation of the nucleobase relative to the parent adenosine (Figure 11B). There is a steric clash between the TNA adenine at position 2 and the amide moiety of the N562 side chain (Figure 11B). Unlike in the parent complex where there is a hydrogen bond between the amide NH and N3 of the adenine, the short contact with TNA at position 2 involves the C2 atom as a result of the different orientation of the base (Figure 11D). This altered interaction may contribute to the loss of activity of an siRNA with TNA incorporated at position 2 of the antisense strand. When the TNA is located at position 3, the slight rotation of the TNA adenine moiety does not affect interactions with Ago2, and stacking with the adjacent residues is maintained as is the

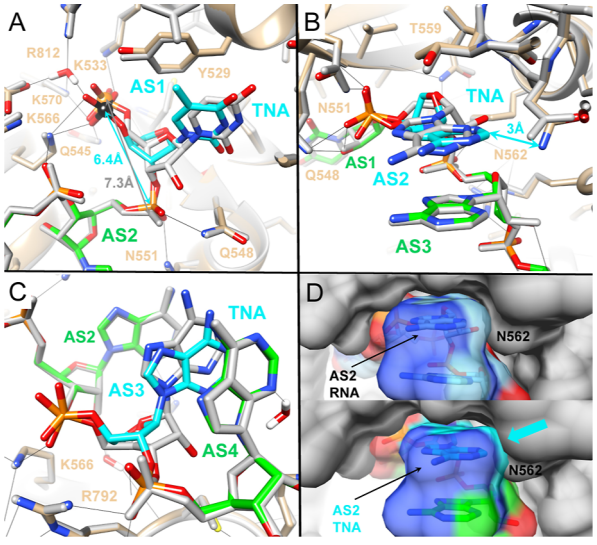

Figure 11. Modeling of siRNA antisense strands modified with TNA bound to Ago2. (A–C) In the complexes, TNA nucleotides at positions (A) 1, (B) 2, and (C) 3 are highlighted with carbon atoms colored in cyan. The remainder of the RNA strand is shown with carbon, nitrogen, oxygen, and phosphorus atoms colored in green, blue, red, and orange, respectively. Ago2 is depicted in the ribbon mode and is colored in tan with side chain atoms colored by atom. Selected Ago2 side chains are labeled and hydrogen bonds are drawn with thin solid lines. (D) Surface models of the parent (top) and TNA-modified (bottom) complexes illustrating the slightly different orientations of the RNA and TNA bases at position 2, which result in a tight contact with N562 in the latter case (cyan arrow).

phosphate–phosphate spacing (Figure 11C). Moreover, the 2′-hydroxyl group at position 3 in the parent complex is not involved in hydrogen bonding with an Ago2 side or main chain atom.

Modification of position 11 of the sense strand with TNA inhibited silencing. Ago2 cleaves the sense strand of the siRNA duplex, and the resulting fragments are released from RISC to enable pairing between the antisense strand and the mRNA target.[58] This cleavage occurs between nucleotides 9 and 10. A PS linkage at position 10 inhibits sense strand cleavage and

https://doi.org/10.1021/jacs.3c04744
J. Am. Chem. Soc. XXXX, XXX, XXX−XXX

slows dissociation of the two siRNA strands, thereby hampering RNAi activity. In crystal structures of human Ago2 in complex with siRNA duplexes, the sense strand is visible up to position 12, but the strand is not lined up for cleavage at the active site and the two required Mg^{2+} ions are missing.[10] In the crystal structure of the complex between *Thermus thermophilus* Ago2 and a DNA sense strand and an antisense RNA strand, multiple lysine and arginine residues engage in contact with the backbone of the sense strand. Inserting a TNA residue at position 11 of the sense strand destabilizes the siRNA duplex and likely introduces a slight conformational change that interferes with cleavage of the sense strand inhibiting subsequent steps in the RNAi pathway.

We also modeled siRNAs with TNA nucleotides at positions 6 and 7 of the antisense strand in complexes with Ago2 using UCSF Chimera[55] for building and Amber[57] for refinement. To build the model with TNA at position 6, we relied on the crystal structure of Ago2 bound to an siRNA duplex as the starting complex (PDB ID 4W5T).[59] The roll bend between base pairs 6 and 7 in this complex is stabilized by amino acids I365 and Q757 and results in short distances of 5.6−5.9 Å between adjacent phosphate groups (Figure 12A). Thus, a TNA residue with its shorter backbone at position 6 matches the tight phosphate−phosphate distance naturally. The situation in the crystal structure of the complex between Ago2 and miR-20a (PDB ID 4F3T) is quite similar.[56] The conformation of the RNA single strand in that complex is characterized by a kink between positions 6 and 7 of the antisense strand with splaying of bases that is aided by I365 (Figure 12B). This results in a phosphate−phosphate spacing of approximately 5.5 Å between positions 7 and 8, a distance that fits the shorter backbone of TNA perfectly. Using just the 5′(3′) and 3′(2′) phosphate atoms as well as the nucleobase atoms for overlaying the TNA-A at position 7 on the crystal structure of miR-20a gives a very good fit with a continuous backbone (Figure 12B). In sum, our modeling studies demonstrate that TNA at positions 6 and 7 of the antisense strand can conformationally pre-organize the siRNA antisense strand and facilitate the local kink in the seed region when the RNA is bound by Ago2. This conformational feature contributes to the mitigation of off-target effects relative to the parent siRNA both in cell-based assays and in rodents.

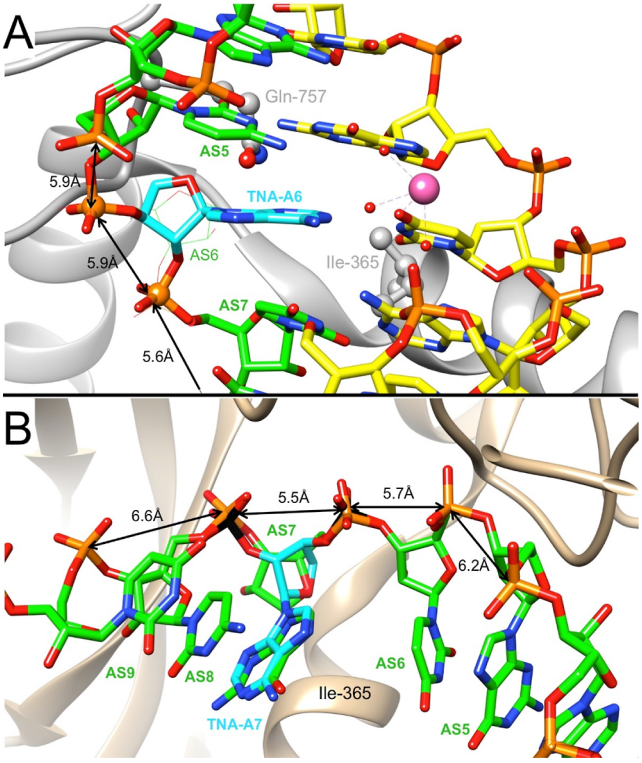

Figure 12. Structural basis of activity gains with siRNAs modified with TNA residues in the seed region. (A) Overlay of TNA-A with A at position 6 of the antisense strand in the crystal structure of human Ago2 in complex with an siRNA duplex (PDB ID 4W5T). The orientation of the parent residue at position 6 is shown with thin lines and TNA phosphorus atoms are highlighted as orange spheres. (B) Overlay of TNA-A with G at position 7 of the antisense strand in the crystal structure of Ago2 in complex with miR-20a (PDB ID 4F3T). TNA phosphorus atoms are highlighted as black spheres. In both panels, carbon atoms of the antisense strand, sense strand, and TNA residues are colored in green, yellow, and cyan, respectively, and selected phosphate−phosphate distances in the backbone of the antisense strands are indicated.

CONCLUSIONS

In this study, we evaluated the positional effect of the TNA modification on the biophysical and biological properties of siRNA duplexes. As previously demonstrated, single incorporation of TNA provides significant stabilization against nuclease cleavage.[30] More importantly, the nuclease resistance resulting from a TNA incorporation was superior to not only 2′-F but also 2′-*O*Me. At present, these modifications are the two industry standards for therapeutic siRNAs. As expected, the incorporation of TNA into RNA or RNA-like duplexes led to a significant thermal destabilization due to the short internucleotide linkage of TNA. The destabilization of the RNA duplex due to incorporation of a TNA residue likely contributed to the observed off-target mitigation observed upon TNA incorporation into the seed regions of the antisense strand of the siRNA. With exceptions of position 2 of the antisense strand and position 11 of the sense strand, a single TNA did not considerably impair silencing activity in cell-based assays or in mice. Interestingly, when incorporated at the 5′ terminus of the antisense strand with or without a phosphate, the RNAi activity was only slightly compromised relative to the parent siRNA. This suggests that the TNA residue serves as a kinase substrate. Data obtained from crystallographic analysis of an RNA duplex containing a TNA residue and molecular modeling indicate that TNA is well accommodated in the duplex bound to Ago2. The results reported here suggest that TNA nucleotides increase potency and duration of action of siRNAs and mitigate off-target effects and thus will likely enhance the safety of siRNAs. Our data indicate that TNA-containing siRNAs warrant further investigation in preclinical and clinical models of disease for effective gene silencing.

ASSOCIATED CONTENT

Data Availability Statement

Structural factors and coordinates for the crystal structure of the modified RNA octamer (Br5C)GAAU(T)CG have been deposited in the Protein Data Bank http://www.rcsb.org with access code 8SKQ.

Supporting Information

The Supporting Information is available free of charge at https://pubs.acs.org/doi/10.1021/jacs.3c04744.

Experimental section, MS analysis of oligonucleotides, additional thermal denaturation data, exonuclease degra-

https://doi.org/10.1021/jacs.3c04744
J. Am. Chem. Soc. XXXX, XXX, XXX−XXX

dation plots, in vitro IC_{50} data, and ^{1}H and ^{13}C spectra for 5-methylcytidine TNA building block (PDF)

AUTHOR INFORMATION

Corresponding Author

Muthiah Manoharan − *Alnylam Pharmaceuticals, Cambridge, Massachusetts 02142, United States;* orcid.org/0000-0002-7931-1172; Email: mmanoharan@alnylam.com

Authors

Shigeo Matsuda − *Alnylam Pharmaceuticals, Cambridge, Massachusetts 02142, United States*

Saikat Bala − *Department of Pharmaceutical Sciences, University of California, Irvine, California 92697-3958, United States;* orcid.org/0000-0002-5285-4476

Jen-Yu Liao − *Department of Pharmaceutical Sciences, University of California, Irvine, California 92697-3958, United States*

Dhrubajyoti Datta − *Alnylam Pharmaceuticals, Cambridge, Massachusetts 02142, United States*

Atsushi Mikami − *Alnylam Pharmaceuticals, Cambridge, Massachusetts 02142, United States*

Lauren Woods − *Alnylam Pharmaceuticals, Cambridge, Massachusetts 02142, United States*

Joel M. Harp − *Department of Biochemistry, School of Medicine, Vanderbilt University, Nashville, Tennessee 37232-0146, United States*

Jason A. Gilbert − *Alnylam Pharmaceuticals, Cambridge, Massachusetts 02142, United States*

Anna Bisbe − *Alnylam Pharmaceuticals, Cambridge, Massachusetts 02142, United States*

Rajar M. Manoharan − *Alnylam Pharmaceuticals, Cambridge, Massachusetts 02142, United States*

MaryBeth Kim − *Alnylam Pharmaceuticals, Cambridge, Massachusetts 02142, United States*

Christopher S. Theile − *Alnylam Pharmaceuticals, Cambridge, Massachusetts 02142, United States*

Dale C. Guenther − *Alnylam Pharmaceuticals, Cambridge, Massachusetts 02142, United States*

Yongfeng Jiang − *Alnylam Pharmaceuticals, Cambridge, Massachusetts 02142, United States*

Saket Agarwal − *Alnylam Pharmaceuticals, Cambridge, Massachusetts 02142, United States;* orcid.org/0000-0002-1681-2842

Rajanikanth Maganti − *Alnylam Pharmaceuticals, Cambridge, Massachusetts 02142, United States*

Mark K. Schlegel − *Alnylam Pharmaceuticals, Cambridge, Massachusetts 02142, United States;* orcid.org/0000-0002-0127-608X

Ivan Zlatev − *Alnylam Pharmaceuticals, Cambridge, Massachusetts 02142, United States*

Klaus Charisse − *Alnylam Pharmaceuticals, Cambridge, Massachusetts 02142, United States*

Kallanthottathil G. Rajeev − *Alnylam Pharmaceuticals, Cambridge, Massachusetts 02142, United States*

Adam Castoreno − *Alnylam Pharmaceuticals, Cambridge, Massachusetts 02142, United States*

Martin Maier − *Alnylam Pharmaceuticals, Cambridge, Massachusetts 02142, United States*

Maja M. Janas − *Alnylam Pharmaceuticals, Cambridge, Massachusetts 02142, United States*

Martin Egli − *Department of Biochemistry, School of Medicine, Vanderbilt University, Nashville, Tennessee 37232-0146, United States;* orcid.org/0000-0003-4145-356X

John C. Chaput − *Department of Pharmaceutical Sciences, University of California, Irvine, California 92697-3958, United States;* orcid.org/0000-0003-1393-135X

Complete contact information is available at: https://pubs.acs.org/10.1021/jacs.3c04744

Notes

The authors declare no competing financial interest.

ACKNOWLEDGMENTS

We are grateful to our colleagues Mollie Plekan for RNA-seq sample preparation, Dan Berman for RNA-seq analysis, Bangyi Ma for clinical pathology analysis, Lauren Moran for rat toxicology study execution, Brenda Carito and Paul Gedman for histology processing, Julia Varao for sample management, and Joseph Berry for advice regarding RNA-seq experiments. This research used resources of the Advanced Photon Source, a U.S. Department of Energy (DOE) Office of Science User Facility operated for the DOE Office of Science by Argonne National Laboratory under contract no. DE-AC02-06CH11357. Use of the LS-CAT Sector 21 was supported by the Michigan Economic Development Corporation and the Michigan Technology Tri-Corridor (grant 085P1000817). We gratefully acknowledge Zdzislaw Wawrzak at LS-CAT for help with X-ray diffraction data collection and processing.

DEDICATION

We dedicate this work to the great life of Professor Albert Eschenmoser (August 5, 1925−July 14, 2023) for his numerous contributions to chemistry including the invention of TNA.[23,60]

REFERENCES

(1) Akinc, A.; Maier, M. A.; Manoharan, M.; Fitzgerald, K.; Jayaraman, M.; Barros, S.; Ansell, S.; Du, X.; Hope, M. J.; Madden, T. D.; Mui, B. L.; Semple, S. C.; Tam, Y. K.; Ciufolini, M.; Witzigmann, D.; Kulkarni, J. A.; van der Meel, R.; Cullis, P. R. The Onpattro story and the clinical translation of nanomedicines containing nucleic acid-based drugs. *Nat. Nanotechnol.* **2019**, *14*, 1084−1087.

(2) Balwani, M.; Sardh, E.; Ventura, P.; Peiró, P. A.; Rees, D. C.; Stölzel, U.; Bissell, D. M.; Bonkovsky, H. L.; Windyga, J.; Anderson, K. E.; Parker, C.; Silver, S. M.; Keel, S. B.; Wang, J.-D.; Stein, P. E.; Harper, P.; Vassiliou, D.; Wang, B.; Phillips, J.; Ivanova, A.; Langendonk, J. G.; Kauppinen, R.; Minder, E.; Horie, Y.; Penz, C.; Chen, J.; Liu, S.; Ko, J. J.; Sweetser, M. T.; Garg, P.; Vaishnaw, A.; Kim, J. B.; Simon, A. R.; Gouya, L. Phase 3 Trial of RNAi Therapeutic Givosiran for Acute Intermittent Porphyria. *N. Engl. J. Med.* **2020**, *382*, 2289−2301.

(3) Chan, A.; Liebow, A.; Yasuda, M.; Gan, L.; Racie, T.; Maier, M.; Kuchimanchi, S.; Foster, D.; Milstein, S.; Charisse, K.; Sehgal, A.; Manoharan, M.; Meyers, R.; Fitzgerald, K.; Simon, A.; Desnick, R. J.; Querbes, W. Preclinical Development of a Subcutaneous ALAS1 RNAi Therapeutic for Treatment of Hepatic Porphyrias Using Circulating RNA Quantification. *Mol. Ther.—Nucleic Acids* **2015**, *4*, No. e263.

(4) Liebow, A.; Li, X.; Racie, T.; Hettinger, J.; Bettencourt, B. R.; Najafian, N.; Haslett, P.; Fitzgerald, K.; Holmes, R. P.; Erbe, D.; Querbes, W.; Knight, J. An Investigational RNAi Therapeutic Targeting Glycolate Oxidase Reduces Oxalate Production in Models of Primary Hyperoxaluria. *J. Am. Soc. Nephrol.* **2017**, *28*, 494−503.

(5) Raal, F. J.; Kallend, D.; Ray, K. K.; Turner, T.; Koenig, W.; Wright, R. S.; Wijngaard, P. L. J.; Curcio, D.; Jaros, M. J.; Leiter, L. A.; Kastelein, J. J. P. Inclisiran for the Treatment of Heterozygous Familial Hypercholesterolemia. *N. Engl. J. Med.* **2020**, *382*, 1520−1530.

https://doi.org/10.1021/jacs.3c04744
J. Am. Chem. Soc. XXXX, XXX, XXX−XXX

(6) Ray, K. K.; Wright, R. S.; Kallend, D.; Koenig, W.; Leiter, L. A.; Raal, F. J.; Bisch, J. A.; Richardson, T.; Jaros, M.; Wijngaard, P. L. J.; Kastelein, J. J. P. Two Phase 3 Trials of Inclisiran in Patients with Elevated LDL Cholesterol. *N. Engl. J. Med.* **2020**, *382*, 1507−1519.
(7) Fitzgerald, K.; White, S.; Borodovsky, A.; Bettencourt, B. R.; Strahs, A.; Clausen, V.; Wijngaard, P.; Horton, J. D.; Taubel, J.; Brooks, A.; Fernando, C.; Kauffman, R. S.; Kallend, D.; Vaishnaw, A.; Simon, A. A Highly Durable RNAi Therapeutic Inhibitor of PCSK9. *N. Engl. J. Med.* **2017**, *376*, 41−51.
(8) Egli, M.; Manoharan, M. Re-Engineering RNA Molecules into Therapeutic Agents. *Acc. Chem. Res.* **2019**, *52*, 1036−1047.
(9) Corey, D. R.; Damha, M. J.; Manoharan, M. Challenges and Opportunities for Nucleic Acid Therapeutics. *Nucleic Acid Ther.* **2022**, *32*, 8−13.
(10) Egli, M.; Manoharan, M. Chemistry, structure and function of approved oligonucleotide therapeutics. *Nucleic Acids Res.* **2023**, *51*, 2529−2573.
(11) Bumcrot, D.; Manoharan, M.; Koteliansky, V.; Sah, D. W. RNAi therapeutics: a potential new class of pharmaceutical drugs. *Nat. Chem. Biol.* **2006**, *2*, 711−719.
(12) Nair, J. K.; Willoughby, J. L. S.; Chan, A.; Charisse, K.; Alam, M. R.; Wang, Q.; Hoekstra, M.; Kandasamy, P.; Kel'in, A. V.; Milstein, S.; Taneja, N.; O'Shea, J.; Shaikh, S.; Zhang, L.; van der Sluis, R. J.; Jung, M. E.; Akinc, A.; Hutabarat, R.; Kuchimanchi, S.; Fitzgerald, K.; Zimmermann, T.; van Berkel, T. J. C.; Maier, M. A.; Rajeev, K. G.; Manoharan, M. Multivalent N-Acetylgalactosamine-Conjugated siRNA Localizes in Hepatocytes and Elicits Robust RNAi-Mediated Gene Silencing. *J. Am. Chem. Soc.* **2014**, *136*, 16958−16961.
(13) Schlegel, M. K.; Foster, D. J.; Kel'in, A. V.; Zlatev, I.; Bisbe, A.; Jayaraman, M.; Lackey, J. G.; Rajeev, K. G.; Charisse, K.; Harp, J.; Pallan, P. S.; Maier, M. A.; Egli, M.; Manoharan, M. Chirality Dependent Potency Enhancement and Structural Impact of Glycol Nucleic Acid Modification on siRNA. *J. Am. Chem. Soc.* **2017**, *139*, 8537−8546.
(14) Guenther, D. C.; Mori, S.; Matsuda, S.; Gilbert, J. A.; Willoughby, J. L. S.; Hyde, S.; Bisbe, A.; Jiang, Y.; Agarwal, S.; Madaoui, M.; Janas, M. M.; Charisse, K.; Maier, M. A.; Egli, M.; Manoharan, M. Role of a "Magic" Methyl: 2′-Deoxy-2′-α-F-2′-β-C-methyl Pyrimidine Nucleotides Modulate RNA Interference Activity through Synergy with 5′-Phosphate Mimics and Mitigation of Off-Target Effects. *J. Am. Chem. Soc.* **2022**, *144*, 14517−14534.
(15) Allerson, C. R.; Sioufi, N.; Jarres, R.; Prakash, T. P.; Naik, N.; Berdeja, A.; Wanders, L.; Griffey, R. H.; Swayze, E. E.; Bhat, B. Fully 2′-modified oligonucleotide duplexes with improved in vitro potency and stability compared to unmodified small interfering RNA. *J. Med. Chem.* **2005**, *48*, 901−904.
(16) Manoharan, M.; Akinc, A.; Pandey, R. K.; Qin, J.; Hadwiger, P.; John, M.; Mills, K.; Charisse, K.; Maier, M. A.; Nechev, L.; Greene, E. M.; Pallan, P. S.; Rozners, E.; Rajeev, K. G.; Egli, M. Unique Gene-Silencing and Structural Properties of 2′-Fluoro-Modified siRNAs. *Angew. Chem., Int. Ed.* **2011**, *50*, 2284−2288.
(17) Pallan, P. S.; Greene, E. M.; Jicman, P. A.; Pandey, R. K.; Manoharan, M.; Rozners, E.; Egli, M. Unexpected origins of the enhanced pairing affinity of 2′-fluoro-modified RNA. *Nucleic Acids Res.* **2011**, *39*, 3482−3495.
(18) Patra, A.; Paolillo, M.; Charisse, K.; Manoharan, M.; Rozners, E.; Egli, M. 2′-Fluoro RNA shows increased Watson-Crick H-bonding strength and stacking relative to RNA: evidence from NMR and thermodynamic data. *Angew. Chem., Int. Ed.* **2012**, *51*, 11863−11866.
(19) Kenski, D. M.; Cooper, A. J.; Li, J. J.; Willingham, A. T.; Haringsma, H. J.; Young, T. A.; Kuklin, N. A.; Jones, J. J.; Cancilla, M. T.; McMasters, D. R.; Mathur, M.; Sachs, A. B.; Flanagan, W. M. Analysis of acyclic nucleoside modifications in siRNAs finds sensitivity at position 1 that is restored by 5′-terminal phosphorylation both in vitro and in vivo. *Nucleic Acids Res.* **2009**, *38*, 660−671.
(20) Laursen, M. B.; Pakula, M. M.; Gao, S.; Fluiter, K.; Mook, O. R.; Baas, F.; Langklær, N.; Wengel, S. L.; Wengel, J.; Kjems, J.; Bramsen, J. B. Utilization of unlocked nucleic acid (UNA) to enhance siRNA performance in vitro and in vivo. *Mol. BioSyst.* **2010**, *6*, 862−870.
(21) Kamiya, Y.; Takai, J.; Ito, H.; Murayama, K.; Kashida, H.; Asanuma, H. Enhancement of Stability and Activity of siRNA by Terminal Substitution with Serinol Nucleic Acid (SNA). *ChemBioChem* **2014**, *15*, 2549−2555.
(22) Alagia, A.; Terrazas, M.; Eritja, R. Modulation of the RNA Interference Activity Using Central Mismatched siRNAs and Acyclic Threoninol Nucleic Acids (aTNA) Units. *Molecules* **2015**, *20*, 7602−7619.
(23) Schöning, K. U.; Scholz, P.; Guntha, S.; Wu, X.; Krishnamurthy, R.; Eschenmoser, A. Chemical Etiology of Nucleic Acid Structure: The α-Threofuranosyl-(3′→2′) Oligonucleotide System. *Science* **2000**, *290*, 1347−1351.
(24) Yu, H.; Zhang, S.; Chaput, J. C. Darwinian evolution of an alternative genetic system provides support for TNA as an RNA progenitor. *Nat. Chem.* **2012**, *4*, 183−187.
(25) Whitaker, D.; Powner, M. W. Prebiotic synthesis and triphosphorylation of 3′-amino-TNA nucleosides. *Nat. Chem.* **2022**, *14*, 766−774.
(26) Culbertson, M. C.; Temburnikar, K. W.; Sau, S. P.; Liao, J.-Y.; Bala, S.; Chaput, J. C. Evaluating TNA stability under simulated physiological conditions. *Bioorg. Med. Chem. Lett.* **2016**, *26*, 2418−2421.
(27) Chaput, J. C. Redesigning the Genetic Polymers of Life. *Acc. Chem. Res.* **2021**, *54*, 1056−1065.
(28) Nikoomanzar, A.; Chim, N.; Yik, E. J.; Chaput, J. C. Engineering polymerases for applications in synthetic biology. *Q. Rev. Biophys.* **2020**, *53*, No. e8.
(29) Dunn, M. R.; McCloskey, C. M.; Buckley, P.; Rhea, K.; Chaput, J. C. Generating biologically stable TNA aptamers that function with high affinity and thermal stability. *J. Am. Chem. Soc.* **2020**, *142*, 7721−7724.
(30) McCloskey, C. M.; Li, Q.; Yik, E. J.; Chim, N.; Ngor, A. K.; Medina, E.; Grubisic, I.; Co Ting Keh, L.; Poplin, R.; Chaput, J. C. Evolution of Functionally Enhanced alpha-l-Threofuranosyl Nucleic Acid Aptamers. *ACS Synth. Biol.* **2021**, *10*, 3190−3199.
(31) Li, X.; Li, Z.; Yu, H. Selection of threose nucleic acid aptamers to block PD-1/PD-L1 interaction for cancer immunotherapy. *Chem. Commun.* **2020**, *56*, 14653−14656.
(32) Wang, Y.; Wang, Y.; Song, D.; Sun, X.; Zhang, Z.; Li, X.; Li, Z.; Yu, H. A Threose Nucleic Acid Enzyme with RNA Ligase Activity. *J. Am. Chem. Soc.* **2021**, *143*, 8154−8163.
(33) Wang, Y.; Wang, Y.; Song, D.; Sun, X.; Li, Z.; Chen, J. Y.; Yu, H. An RNA-cleaving threose nucleic acid enzyme capable of single point mutation discrimination. *Nat. Chem.* **2022**, *14*, 350−359.
(34) Yang, K.; McCloskey, C. M.; Chaput, J. C. Reading and Writing Digital Information in TNA. *ACS Synth. Biol.* **2020**, *9*, 2936−2942.
(35) Lu, X.; Wu, X.; Wu, T.; Han, L.; Liu, J.; Ding, B. Efficient construction of a stable linear gene based on a TNA loop modified primer pair for gene delivery. *Chem. Commun.* **2020**, *56*, 9894−9897.
(36) Liu, L. S.; Leung, H. M.; Tam, D. Y.; Lo, T. W.; Wong, S. W.; Lo, P. K. α-l-Threose Nucleic Acids as Biocompatible Antisense Oligonucleotides for Suppressing Gene Expression in Living Cells. *ACS Appl. Mater. Interfaces* **2018**, *10*, 9736−9743.
(37) Wang, F.; Liu, L. S.; Lau, C. H.; Han Chang, T. J.; Tam, D. Y.; Leung, H. M.; Tin, C.; Lo, P. K. Synthetic alpha-l-Threose Nucleic Acids Targeting BcL-2 Show Gene Silencing and in Vivo Antitumor Activity for Cancer Therapy. *ACS Appl. Mater. Interfaces* **2019**, *11*, 38510−38518.
(38) Wang, Y.; Nguyen, K.; Spitale, R. C.; Chaput, J. C. A biologically stable DNAzyme that efficiently silences gene expression in cells. *Nat. Chem.* **2021**, *13*, 319−326.
(39) Nguyen, K.; Wang, Y. J.; England, W. E.; Chaput, J. C.; Spitale, R. C. Allele-Specific RNA Knockdown with a Biologically Stable and Catalytically Efficient XNAzyme. *J. Am. Chem. Soc.* **2021**, *143*, 4519−4523.
(40) Wang, F.; Liu, L. S.; Li, P.; Lau, C. H.; Leung, H. M.; Chin, Y. R.; Tin, C.; Lo, P. K. Cellular uptake, tissue penetration, biodistribution, and biosafety of threose nucleic acids: Assessing in vitro and in vivo delivery. *Mater. Today Bio* **2022**, *15*, 100299.

https://doi.org/10.1021/jacs.3c04744
J. Am. Chem. Soc. XXXX, XXX, XXX−XXX

(41) Sau, S. P.; Fahmi, N. E.; Liao, J.-Y.; Bala, S.; Chaput, J. C. A Scalable Synthesis of α-l-Threose Nucleic Acid Monomers. *J. Org. Chem.* **2016**, *81*, 2302−2307.
(42) Zhang, S.; Chaput, J. C. Synthesis of threose nucleic acid (TNA) phosphoramidite monomers and oligonucleotide polymers. *Curr. Protoc. Nucleic Acid Chem.* **2012**, *50*, 4.51.1.
(43) Schlegel, M. K.; Matsuda, S.; Brown, C. R.; Harp, J. M.; Barry, J.; Berman, D.; Castoreno, A.; Schofield, S.; Szeto, J.; Manoharan, M.; Charissé, K.; Egli, M.; Maier, M. A. Overcoming GNA/RNA base-pairing limitations using isonucleotides improves the pharmacodynamic activity of ESC+ GalNAc-siRNAs. *Nucleic Acids Res.* **2021**, *49*, 10851−10867.
(44) Schlegel, M. K.; Janas, M. M.; Jiang, Y.; Barry, J. D.; Davis, W.; Agarwal, S.; Berman, D.; Brown, C. R.; Castoreno, A.; LeBlanc, S.; Liebow, A.; Mayo, T.; Milstein, S.; Nguyen, T.; Shulga-Morskaya, S.; Hyde, S.; Schofield, S.; Szeto, J.; Woods, L.; Yilmaz, V.; Manoharan, M.; Egli, M.; Charissé, K.; Sepp-Lorenzino, L.; Haslett, P.; Fitzgerald, K.; Jadhav, V.; Maier, M. A. From bench to bedside: Improving the clinical safety of GalNAc−siRNA conjugates using seed-pairing destabilization. *Nucleic Acids Res.* **2022**, *50*, 6656−6670.
(45) Akabane-Nakata, M.; Erande, N. D.; Kumar, P.; Degaonkar, R.; Gilbert, J. A.; Qin, J.; Mendez, M.; Woods, L. B.; Jiang, Y.; Janas, M. M.; O'Flaherty, D. K.; Zlatev, I.; Schlegel, M. K.; Matsuda, S.; Egli, M.; Manoharan, M. siRNAs containing 2-fluorinated Northern-methanocarbacyclic (2-F-NMC) nucleotides: in vitro and in vivo RNAi activity and inability of mitochondrial polymerases to incorporate 2-F-NMC NTPs. *Nucleic Acids Res.* **2021**, *49*, 2435−2449.
(46) Akabane-Nakata, M.; Kumar, P.; Das, R. S.; Erande, N. D.; Matsuda, S.; Egli, M.; Manoharan, M. Synthesis and Biophysical Characterization of RNAs Containing 2'-Fluorinated Northern Methanocarbacyclic Nucleotides. *Org. Lett.* **2019**, *21*, 1963−1967.
(47) Schwarz, D. S.; Hutvágner, G.; Du, T.; Xu, Z.; Aronin, N.; Zamore, P. D. Asymmetry in the Assembly of the RNAi Enzyme Complex. *Cell* **2003**, *115*, 199−208.
(48) Janas, M. M.; Schlegel, M. K.; Harbison, C. E.; Yilmaz, V. O.; Jiang, Y.; Parmar, R.; Zlatev, I.; Castoreno, A.; Xu, H.; Shulga-Morskaya, S.; Rajeev, K. G.; Manoharan, M.; Keirstead, N. D.; Maier, M. A.; Jadhav, V. Selection of GalNAc-conjugated siRNAs with limited off-target-driven rat hepatotoxicity. *Nat. Commun.* **2018**, *9*, 723.
(49) Agarwal, V.; Bell, G. W.; Nam, J. W.; Bartel, D. P. Predicting effective microRNA target sites in mammalian mRNAs. *Elife* **2015**, *4*, No. e05005.
(50) Wilds, C. J.; Wawrzak, Z.; Krishnamurthy, R.; Eschenmoser, A.; Egli, M. Crystal Structure of a B-Form DNA Duplex Containing (l)-α-Threofuranosyl (3′→2′) Nucleosides: A Four-Carbon Sugar Is Easily Accommodated into the Backbone of DNA. *J. Am. Chem. Soc.* **2002**, *124*, 13716−13721.
(51) Pallan, P. S.; Wilds, C. J.; Wawrzak, Z.; Krishnamurthy, R.; Eschenmoser, A.; Egli, M. Why Does TNA Cross-Pair More Strongly with RNA Than with DNA? An Answer From X-ray Analysis. *Angew. Chem., Int. Ed.* **2003**, *42*, 5893−5895.
(52) Ebert, M.-O.; Mang, C.; Krishnamurthy, R.; Eschenmoser, A.; Jaun, B. The Structure of a TNA−TNA Complex in Solution: NMR Study of the Octamer Duplex Derived from α-(l)-Threofuranosyl-(3′-2′)-CGAATTCG. *J. Am. Chem. Soc.* **2008**, *130*, 15105−15115.
(53) Chim, N.; Shi, C.; Sau, S. P.; Nikoomanzar, A.; Chaput, J. C. Structural basis for TNA synthesis by an engineered TNA polymerase. *Nat. Commun.* **2017**, *8*, 1810.
(54) Zhang, W.; Kim, S. C.; Tam, C. P.; Lelyveld, V. S.; Bala, S.; Chaput, J. C.; Szostak, J. W. Structural interpretation of the effects of threo-nucleotides on nonenzymatic template-directed polymerization. *Nucleic Acids Res.* **2021**, *49*, 646−656.
(55) Pettersen, E. F.; Goddard, T. D.; Huang, C. C.; Couch, G. S.; Greenblatt, D. M.; Meng, E. C.; Ferrin, T. E. UCSF Chimera—A visualization system for exploratory research and analysis. *J. Comput. Chem.* **2004**, *25*, 1605−1612.
(56) Elkayam, E.; Kuhn, C.-D.; Tocilj, A.; Haase, A.; Greene, E. M.; Hannon, G. J.; Joshua-Tor, L. The Structure of Human Argonaute-2 in Complex with miR-20a. *Cell* **2012**, *150*, 100−110.
(57) Case, D.; Babin, V.; Berryman, J.; Betz, R.; Cai, Q.; Cerutti, D.; Cheatham, T.; Darden, T.; Duke, R.; Gohlke, H.; Götz, A.; Gusarov, S.; Homeyer, N.; Janowski, P.; Kaus, J.; Kolossváry, I.; Kovalenko, A.; Lee, T.-S.; Legrand, S.; Kollman, P. *Amber*, 2014.
(58) Matranga, C.; Tomari, Y.; Shin, C.; Bartel, D. P.; Zamore, P. D. Passenger-Strand Cleavage Facilitates Assembly of siRNA into Ago2-Containing RNAi Enzyme Complexes. *Cell* **2005**, *123*, 607−620.
(59) Schirle, N. T.; Sheu-Gruttadauria, J.; MacRae, I. J. Structural basis for microRNA targeting. *Science* **2014**, *346*, 608−613.
(60) Schreiber, S., "Albert Eschenmoser taught us whole new ways to think about organic chemistry − from orbitals, to mechanisms, to syntheses, to life processes, and eventually even to the origins of life. His passing marks the end of an era defined by his intellectual brilliance". Twitter, July 16, 2023.

https://doi.org/10.1021/jacs.3c04744
J. Am. Chem. Soc. XXXX, XXX, XXX−XXX